Multiphysics 2010, Kumamoto, Japan

Multiphysics Computational Simulations Challenges and opportunities

Zoran Ren

University of Maribor
Faculty of Mechanical Engineering
Slovenia

What is MULTIPHYSICS?

MULTIPHYSICS = multiple simultaneous physical phenomena interaction between two or more physical systems.

Multiphysics Computational Simulations = solving coupled systems of partial differential equations that mathematically model the behaviour of interacting physical systems.

Coupled Systems = when an independent solution of one system is impossible without a simultaneous solution of the others.

Types of MULTIPHYSICS problems

More common and mature analyses of coupled physics:

- **fluid–structure (fluid–solid) interaction**,
- **thermal–mechanical interaction**,
- **electric–thermal interaction**.

New and emerging types of coupled physics analyses :

- **all above interactions combined** on
- **nano and micro level analyses (e.g. MEMS)** and
- **extremely large scale (e.g. Universe),**
- **chemical reactions,**
- **electromagnetic fluids, bioengineering etc**.

Computational solution techniques

Two numerical techniques for solving coupled problems are available:

- **sequentialy-coupled solution process** and
- **directly-coupled solution process.**

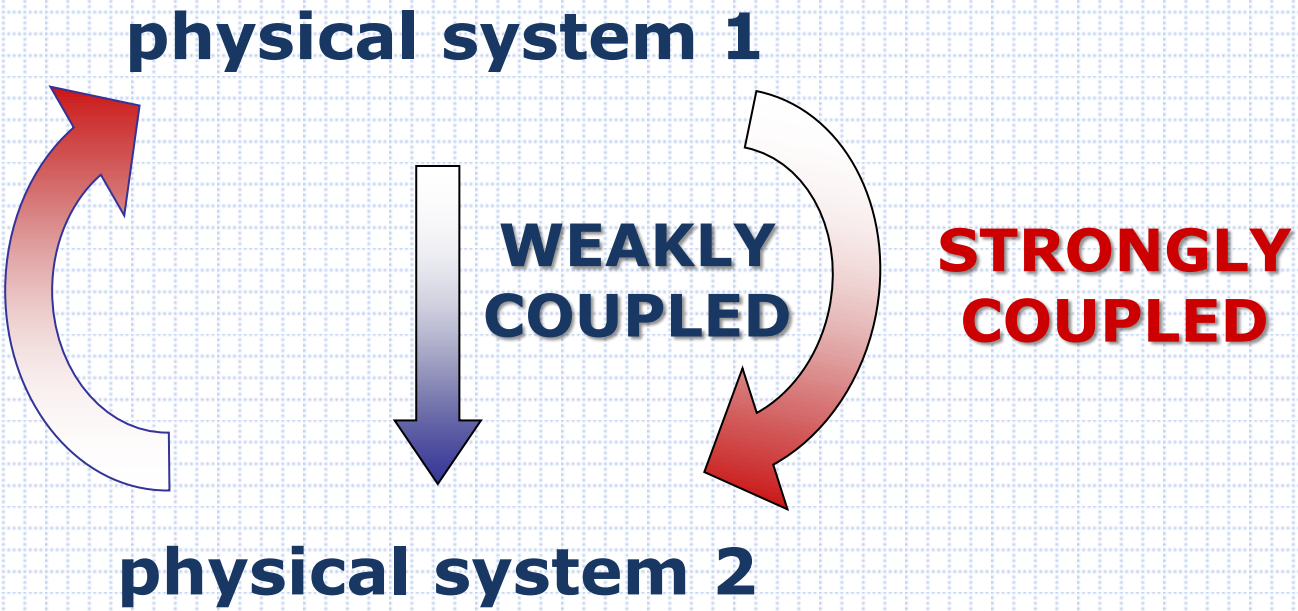

Computational simulations

In the past: separate analyses of each phenomenon individually and consequently, many manual file transfers and data exchanges required; computational analyses cumbersome, error-prone, and time-consuming; often took days or weeks to perform.

Today: multiphysics software packages automatically combine the effects of two or more interrelated physical phenomena, automatically manage the exchange of data and perform information transfers; analyses reliable and quick; users can complete many more iterations in a given time, and explore a broader range of engineering parameters to obtain more accurate solutions.

Software and Hardware

Software: all mayor engineering simulation software packages now include Multiphysics capabilities with use of either **single discretisation methods (FEM, BEM, FVM, EFGM etc.)** or **multiple discretisation methods** seamlessly combined.

Hardware: multiple processing capabilities required and easily available through use of modern **multi-core CPUs or cluster/cloud computing**; future generations of CPUs, based on electro-chemical operating principles, will forewer change computing as we know it today.

Example case studies

Fluid-Structure Interaction (FSI):

- deformations and stresses in operating mixing vessel,
- fluid filler effect on stiffness of a cellular structure.

Chemical-Fluid-Structure Interaction (CFSI):

- behaviour of cellular structure when subjected to underwater shock wave caused by explosion.

ANALYSIS OF THE MIXING VESSEL

Problem statement

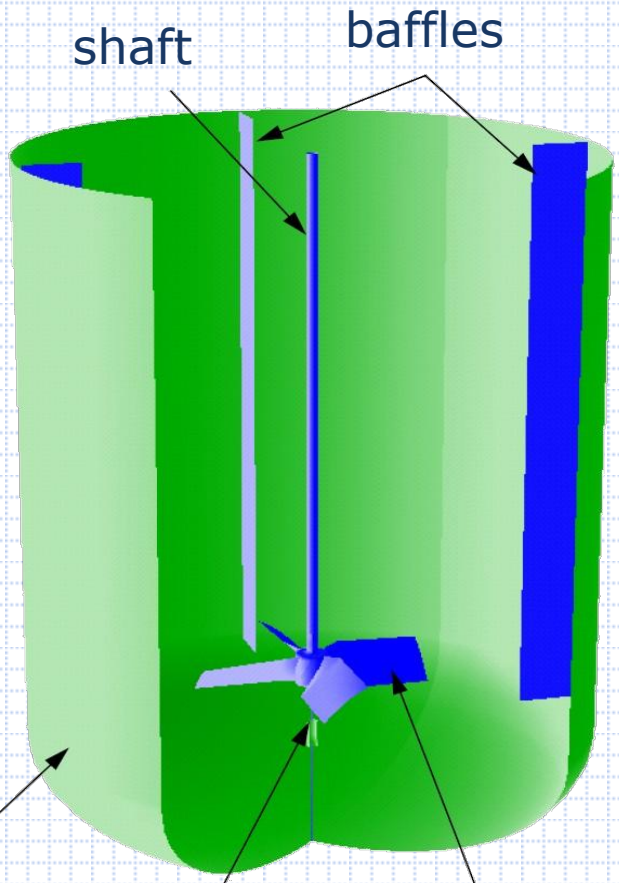

Fluids:
- water
- air

Angular blade speed:	3 s^{-1}
Air injection speed:	5 m/s
Length of the blade:	450 mm
Height of the blade:	290 mm

Computational fluid dynamics:

CFX

Computational solid mechanics:

MSC.visualNastran for Windows

Fluid dynamics relationships

- fundamental equations of the fluid mechanics

$$\frac{D\rho}{Dt} + \rho \cdot \nabla \cdot \mathbf{v} = 0$$ mass equation

$$\rho \cdot \frac{D\mathbf{v}}{Dt} = \rho \cdot \mathbf{f} - \nabla \cdot \boldsymbol{\sigma}$$ momentum equation

$$\rho \cdot \frac{Du}{Dt} = -\frac{\delta q_j}{\delta x_j} + I - p \cdot \frac{\delta v_j}{\delta x_j} + \Phi$$ energy equation

conservation equations

$$\boldsymbol{\sigma} = -p \cdot \boldsymbol{\delta} + 2 \cdot \eta \cdot \boldsymbol{\varepsilon}$$ constitutive equation

- Navier-Stokes equations

$$\rho \cdot \frac{D\mathbf{v}}{Dt} = \rho \cdot \mathbf{f} - \nabla \cdot p + \eta \cdot \nabla^2 \cdot \mathbf{v}$$

- integral form of the Navier-Stokes equations

$$\int_V \frac{\delta(\mathbf{v} \cdot \rho)}{\delta t} \cdot dV + \int_S \mathbf{v} \cdot \rho \cdot \mathbf{v} \cdot \mathbf{n} \cdot dS - \int_V \rho \cdot \mathbf{f} \cdot dV - \int_S \boldsymbol{\sigma} \cdot \mathbf{n} \cdot dS = 0$$

- discretisation with the finite volume method

$$\rho \cdot \frac{\Delta \mathbf{v}_i}{\Delta t} \cdot dV_i + \dot{m}_i \cdot \mathbf{v}_i - \rho \cdot \mathbf{f}_i \cdot V_i + \mathbf{p}_i \cdot S_i - 2 \cdot \eta \cdot \boldsymbol{\varepsilon}_i \cdot S_i = 0$$

Solid mechanics relationships

- fundamental equations of the quasi-static solid mechanics

$\mathbf{L}^T \cdot \boldsymbol{\sigma} + \mathbf{p} = 0$ equilibrium equations

$\boldsymbol{\varepsilon} = \mathbf{L} \cdot \mathbf{u}$ kinematic equations

$\boldsymbol{\sigma} = \mathbf{D} \cdot \boldsymbol{\varepsilon}$ constitutive equations

- weak integral form of the equilibrium equations

$$\int_S \mathbf{t} \cdot dS - \int_V \boldsymbol{\sigma} \cdot dV + \int_V \mathbf{p} \cdot dV = 0$$

- discretisation with the finite element method

$$\underbrace{\int_V \mathbf{B}^T \cdot \mathbf{D}_e \cdot \mathbf{B} \cdot dV}_{\mathbf{K}} \cdot \mathbf{d}_e = \underbrace{\int_{S_t} \mathbf{N}_e^T \cdot \mathbf{t}_e \cdot dS + \int_V \mathbf{N}_e^T \cdot \mathbf{p}_e \cdot dV}_{\mathbf{f}_z}$$

$\mathbf{K}$ stiffness matrix

$\mathbf{f}_z$ force vector

Sequentialy-coupled solution process

interface boundary conditions:

$$\Delta\mathbf{v}\cdot\mathbf{n}=\Delta\mathbf{v}\cdot\mathbf{t}=0$$

$$\mathbf{p}_i=p_i\cdot\mathbf{n}_{fluid}=-p_i\cdot\mathbf{n}_{strucure}$$

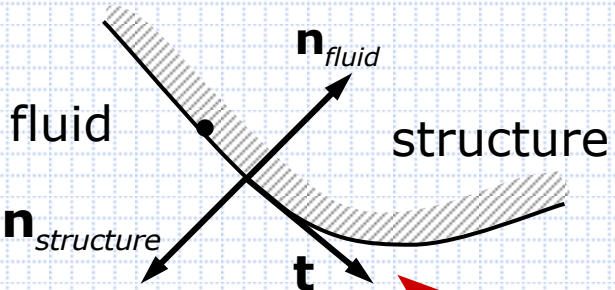

discretised fluid mechanics equation:

$$\rho\cdot\frac{\Delta\mathbf{v}_i}{\Delta t}\cdot dV_i+\dot{m}_i\cdot\mathbf{v}_i-\rho\cdot\mathbf{f}_i\cdot V_i+\mathbf{p}_i\cdot S_i-2\cdot\eta\cdot\boldsymbol{\varepsilon}_i\cdot S_i=0$$

$$\mathbf{p}_i=\frac{-\rho\cdot\frac{\Delta\mathbf{v}_i}{\Delta t}\cdot dV_i-\dot{m}_i\cdot\mathbf{v}_i+\rho\cdot\mathbf{f}_i\cdot V_i+2\cdot\eta\cdot\boldsymbol{\varepsilon}_i\cdot S_i}{S_i}=-\mathbf{t}_e$$

geometry and mesh redefinition for computational fluid dynamics (CFD) analysis

discretised solid mechanics equation:

$$\mathbf{K}_e\cdot\mathbf{d}_e=\int_V\mathbf{N}_e^T\cdot\mathbf{p}_e\cdot dV+\int_{S_t}\mathbf{N}_e^T\cdot\mathbf{t}_e\cdot dS=\int_V\mathbf{N}_e^T\cdot\mathbf{p}_e\cdot dV-\int_{S_t}\mathbf{N}_e^T\cdot\mathbf{p}_i\cdot dS$$

$$\mathbf{d}_e=\mathbf{K}_e^{-1}\cdot\left(\int_V\mathbf{N}_e^T\cdot\mathbf{p}_e\cdot dV-\int_{S_t}\mathbf{N}_e^T\cdot\mathbf{p}_i\cdot dS\right)$$

stresses
strains

CFD Analysis of the Mixing Vessel

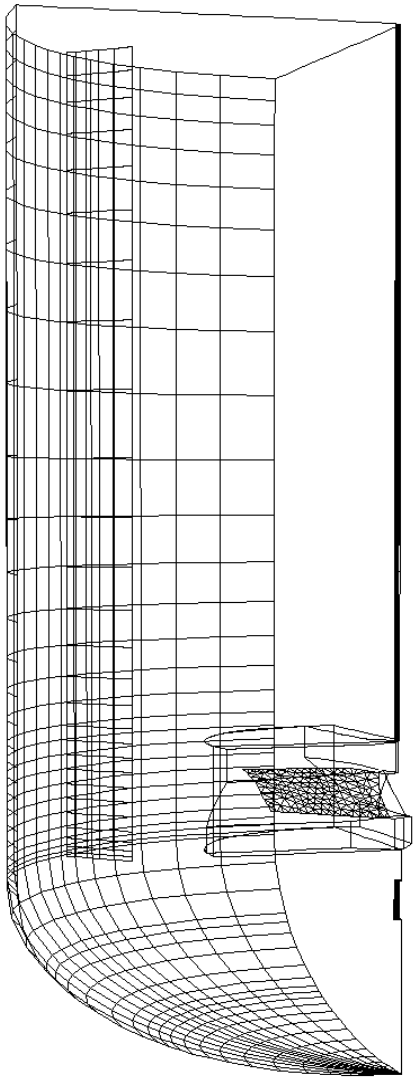

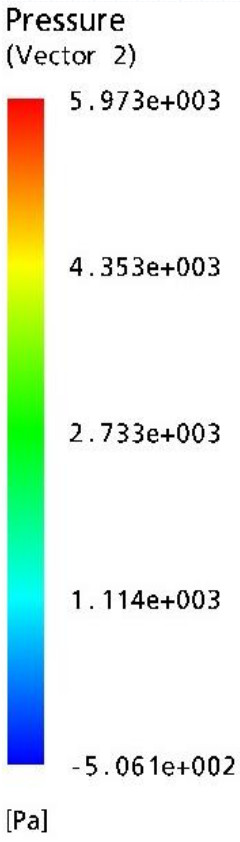

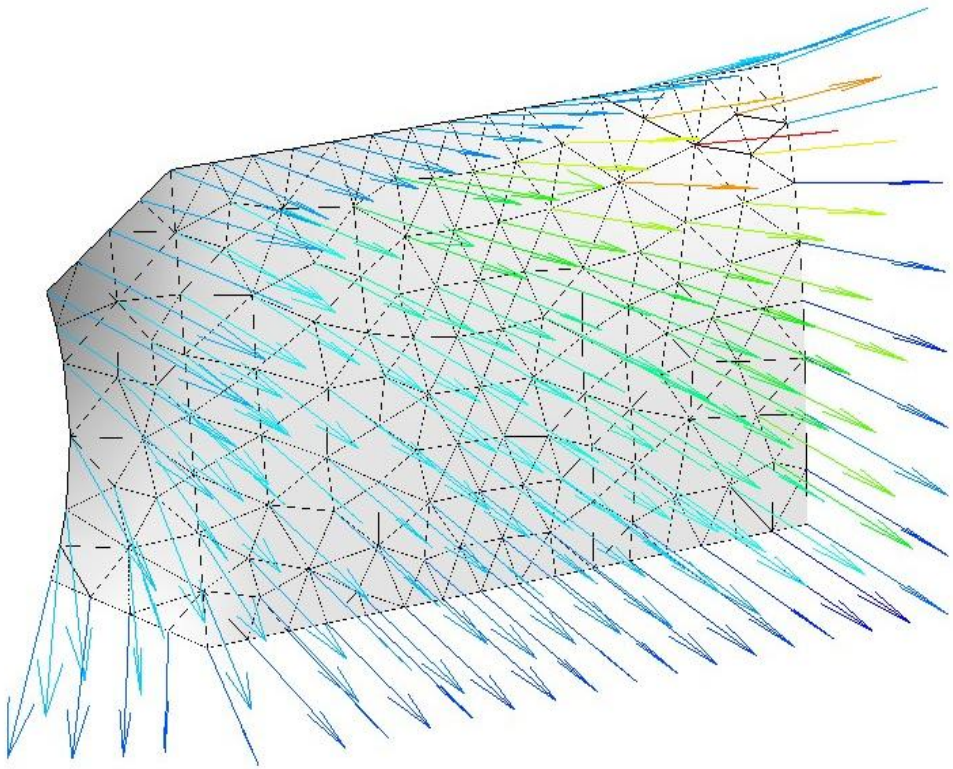

Nodal pressure forces at the blade surface.

Connection between CFX (output data) and MSC/Nastran (input data)

```
#
# CFX-Post data export file
# CFX-5.6 build 2003.04.29-23.00
# Generated on:  2003/09/21 12:36:28
#
# Generated from file: d:\cfxs\Mixer_002.res
#
# Format used:
#     Floats to be displayed with a precision of: 3
#     Variable data will be separated with: ",      "
#     Vector components will be displayed using no brackets to delimit.
#
# Locator Description(s):
#        Blade : BOUNDARY
#
#
# The following variables will be output for all locators:
#     1 - X [m]
#     2 - Y [m]
#     3 - Z [m]
#     4 - Air at 25 C.Force X [N]
#     5 - Air at 25 C.Force Y [N]
#     6 - Air at 25 C.Force Z [N]
#     7 - Water at 25 C.Force X [N]
#     8 - Water at 25 C.Force Y [N]
#     9 - Water at 25 C.Force Z [N]
#

1.866e-01,  2.550e-01, -8.884e-02, 2.812e-03,  -1.276e-05, -2.819e-03, 5.986e-02, -1.464e-03, -6.835e-02
1.866e-01,  2.780e-01, -8.893e-02, -2.301e-05, -1.924e-07, 2.247e-05,  2.416e-02, -9.646e-04, -3.100e-02
2.036e-01,  2.681e-01, -7.193e-02, -9.754e-04, -1.321e-06, 9.594e-04,  4.697e-02, -1.717e-03, -5.895e-02
1.866e-01,  3.011e-01, -8.902e-02, 3.730e-04,  -1.526e-06, -3.734e-04, 3.625e-02, -1.305e-03, -4.492e-02
2.058e-01,  2.902e-01, -6.978e-02, 3.772e-04,  -1.700e-06, -3.915e-04, 1.367e-01, -2.356e-03, -1.526e-01
1.866e-01,  3.701e-01, -8.929e-02, 1.637e-03,  -6.493e-06, -1.642e-03, 1.424e-01, -2.863e-03, -1.611e-01
.
.
.
2.750e-01,  7.500e-02, 9.627e-08,  9.798e-02,  1.625e-03,  -1.508e-01, 2.404e-01, -4.035e-03, -3.582e-01
3.062e-01,  1.217e-01, 2.782e-02,  5.089e-02,  1.045e-02,  -5.940e-02, 2.663e-01, 6.262e-02,  -3.028e-01
2.966e-01,  1.018e-01, 1.653e-02,  1.307e-01,  2.499e-02,  -1.791e-01, 3.568e-01, 6.641e-02,  -4.752e-01
3.125e-01,  7.205e-02, 2.084e-02,  7.644e-02,  2.716e-02,  -1.165e-01, 1.565e-01, 6.176e-02,  -2.361e-01
```

File with output data (CFX)

```
INIT MASTER(S)
ID d:\Solid-Fluid\Primer 03.,MSC.v
SOL SESTATICS
TIME 10000
CEND
  ECHO = NONE
  DISPLACEMENT(PLOT) = ALL
  SPCFORCE(PLOT) = ALL
  OLOAD(PLOT) = ALL
  FORCE(PLOT,CORNER) = ALL
  STRESS(PLOT,CORNER) = ALL
  SPC = 1
  LOAD = 1
BEGIN BULK
$ ***********************************************
$   Written by : MSC.visualNastran for Windows
$   Version    : 2002
$   Modeller   : 8.10
$   Translator : MSC.Nastran
$   From Model : d:\Solid-Fluid\Primer 03.MOD
$   Date       : Mon Sep 08 14:22:50 2003
$ ***********************************************
$
PARAM,POST,-1
PARAM,OGEOM,NO
PARAM,AUTOSPC,YES
PARAM,K6ROT,100.
PARAM,MAXRATIO,1.E+8
PARAM,GRDPNT,0
CORD2C          1       0      0.      0.      0.      0.      0.      1.+MSC.VC1
+MSC.VC1        1.      0.      1.
CORD2S          2       0      0.      0.      0.      0.      0.      1.+MSC.VC2
+MSC.VC2        1.      0.      1.
$ MSC.visualNastran for Windows Load Set 1 : Obremenitev
FORCE           1       1       0       1.0.062672-1.48E-3-7.12E-2
FORCE           1       2       0       1.0.024135-9.65E-4-3.10E-2
.
.
.
FORCE           1     154       0       1. 0.48754  0.0914-0.65425
FORCE           1     155       0       1. 0.232920.088912-0.35259
$ MSC.visualNastran for Windows Constraint Set 1 : Vpetje
SPC1            1  123456     140
SPC1            1  123456     141
SPC1            1  123456     143
SPC1            1  123456     145
SPC1            1  123456     148
SPC1            1  123456     152
SPC1            1  123456     155
$ MSC.visualNastran for Windows Property 1 : Plosca
PSHELL          1       1      5.       1               1               0.
$ MSC.visualNastran for Windows Material 1 : Jeklo
MAT1            1 210000.               0.3      0.      0.      0.
GRID            1       0 0.18661 0.25504-8.88E-2       0
GRID            2       0 0.18661 0.27805-8.89E-2       0
.
.
.
GRID          157       0 0.34014 0.287580.074767       0
GRID          158       0 0.34014 0.287580.074767       0
CTRIA3          1       1      38      69      66
CTRIA3          2       1     144     143     145
.
.
.
CTRIA3        256       1      29      28      72
CTRIA3        257       1      28      72      65
ENDDATA d7c6cfa2
```

File with input data (Nastran)

Connection between CFX (output data) and MSC/Nastran (input data)

CFX

```
1.866e-01,  2.550e-01, -8.884e-02,  2.812e-03, -1.276e-05, -2.819e-03,  5.986e-02, -1.464e-03, -6.835e-02
1.866e-01,  2.780e-01, -8.893e-02, -2.301e-05, -1.924e-07,  2.247e-05,  2.416e-02, -9.646e-04, -3.100e-02
2.036e-01,  2.681e-01, -7.193e-02, -9.754e-04, -1.321e-06,  9.594e-04,  4.697e-02, -1.717e-03, -5.895e-02
1.866e-01,  3.011e-01, -8.902e-02,  3.730e-04, -1.526e-06, -3.734e-04,  3.625e-02, -1.305e-03, -4.492e-02
2.058e-01,  2.902e-01, -6.978e-02,  3.772e-04, -1.700e-06, -3.915e-04,  1.367e-01, -2.356e-03, -1.526e-01
1.866e-01,  3.701e-01, -8.929e-02,  1.637e-03, -6.493e-06, -1.642e-03,  1.424e-01, -2.863e-03, -1.611e-01
1.866e-01,  3.931e-01, -8.938e-02, -9.717e-05,  3.790e-07,  9.708e-05,  1.211e-02, -4.058e-04, -1.792e-02
```

x y z

Nastran

```
GRID            1       0 0.18661 0.25504-8.88E-2       0
GRID            2       0 0.18661 0.27805-8.89E-2       0
```

x y z

determination of the node positions

CFX

```
1.866e-01,  2.550e-01, -8.884e-02,  2.812e-03, -1.276e-05, -2.819e-03,  5.986e-02, -1.464e-03, -6.835e-02
1.866e-01,  2.780e-01, -8.893e-02, -2.301e-05, -1.924e-07,  2.247e-05,  2.416e-02, -9.646e-04, -3.100e-02
2.036e-01,  2.681e-01, -7.193e-02, -9.754e-04, -1.321e-06,  9.594e-04,  4.697e-02, -1.717e-03, -5.895e-02
1.866e-01,  3.011e-01, -8.902e-02,  3.730e-04, -1.526e-06, -3.734e-04,  3.625e-02, -1.305e-03, -4.492e-02
2.058e-01,  2.902e-01, -6.978e-02,  3.772e-04, -1.700e-06, -3.915e-04,  1.367e-01, -2.356e-03, -1.526e-01
1.866e-01,  3.701e-01, -8.929e-02,  1.637e-03, -6.493e-06, -1.642e-03,  1.424e-01, -2.863e-03, -1.611e-01
1.866e-01,  3.931e-01, -8.938e-02, -9.717e-05,  3.790e-07,  9.708e-05,  1.211e-02, -4.058e-04, -1.792e-02
```

x-force (air) y-force (air) z-force (air) x-force (water) y-force (water) z-force (water)

Nastran

```
FORCE,1,1,0,1,6.2671953114E-02,-1.4768094698E-03,-7.1172522847E-02
FORCE,1,2,0,1,2.4134511885E-02,-9.6480049660E-04,-3.0978766561E-02
```

x-force y-force z-force

determination of the loads

FEM Analysis of the blade

- determination of material properties (steel)
- boundary conditions (constraints and loads)

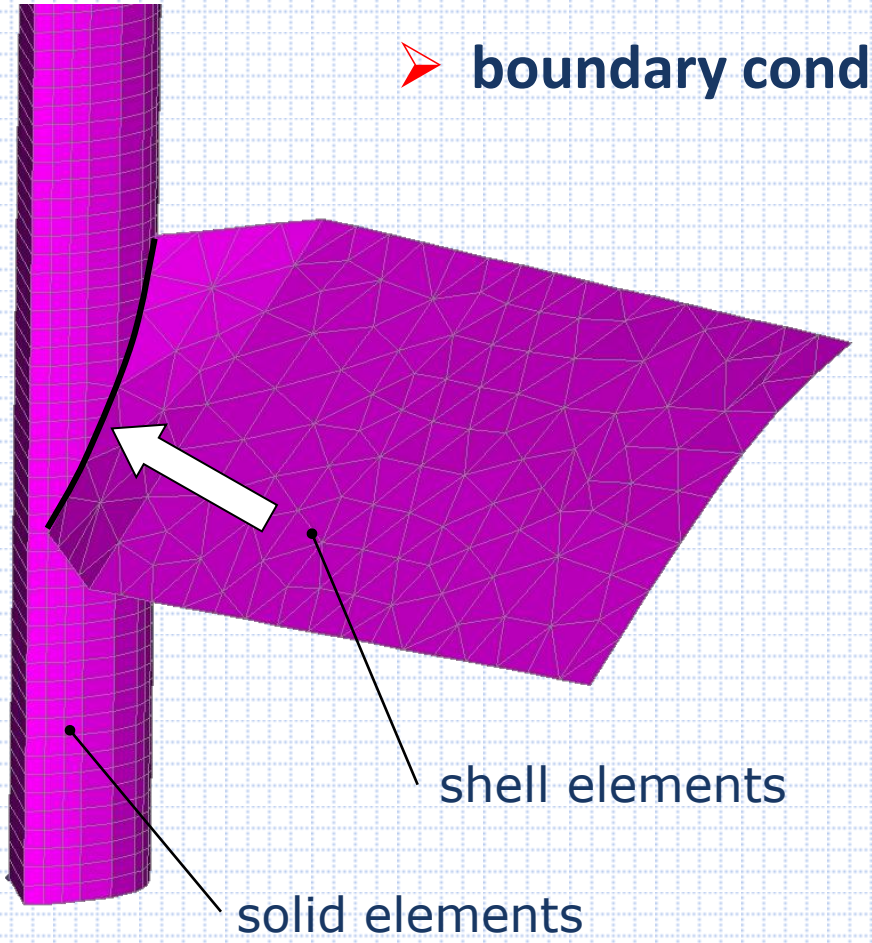

linear quasi-static analysis

ANALYSIS OF THE MIXING VESSEL

Results of the FEM analysis

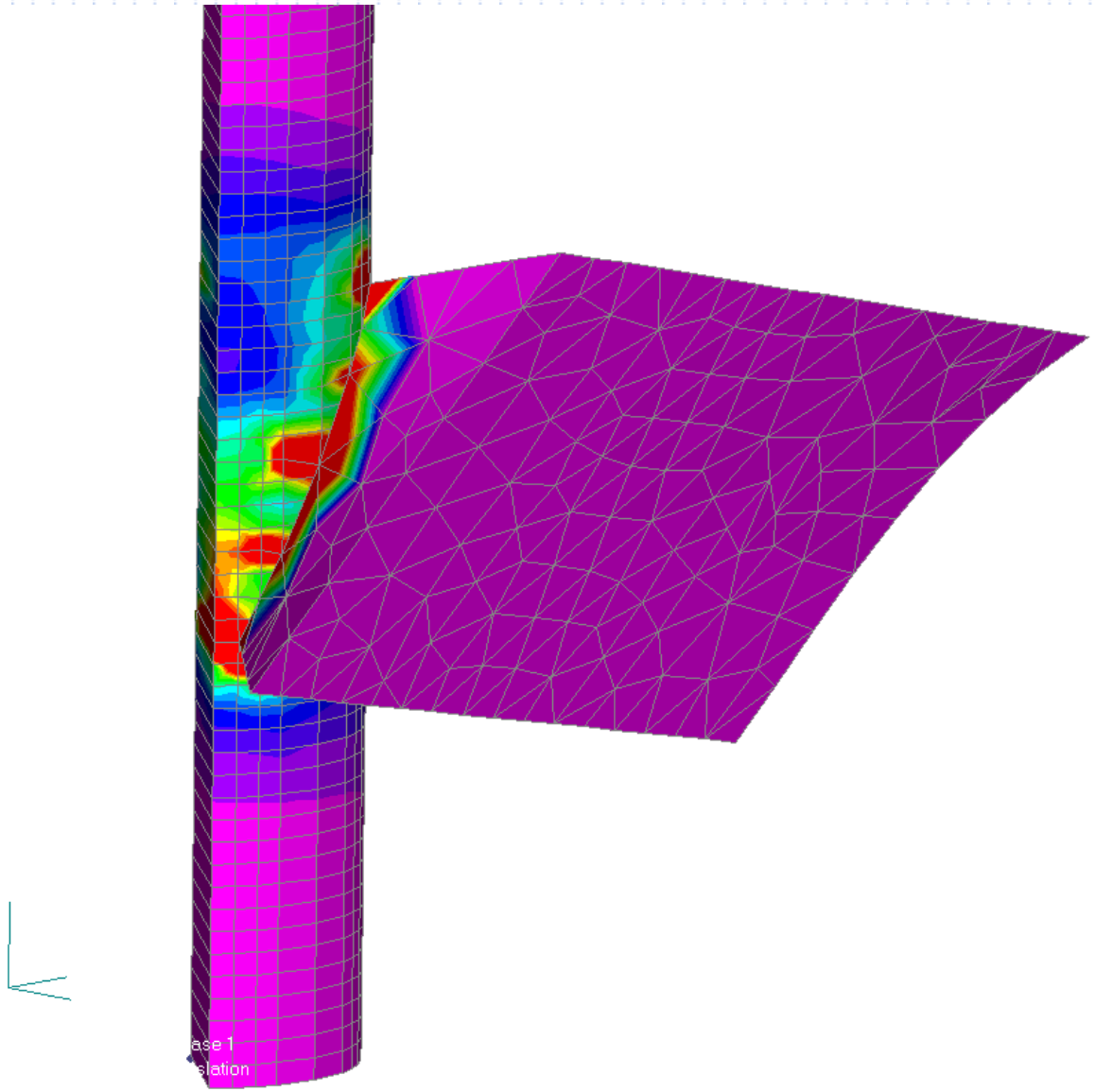

ANALYSIS OF THE MIXING VESSEL

Results of the FEM analysis

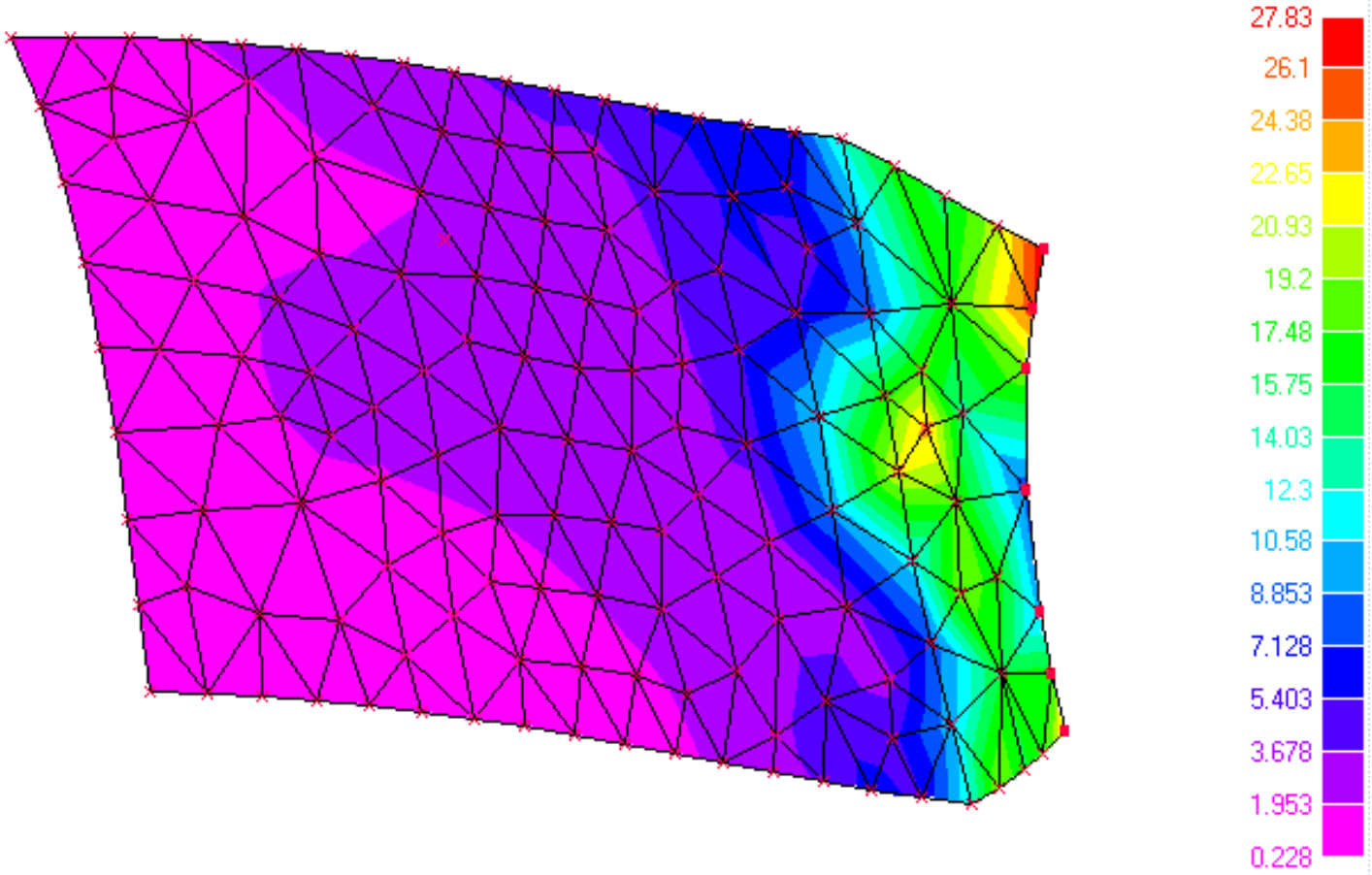

Cellular materials


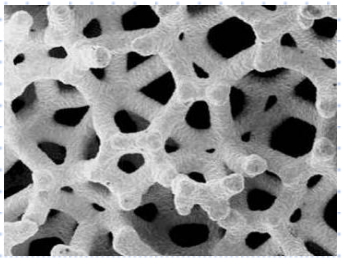
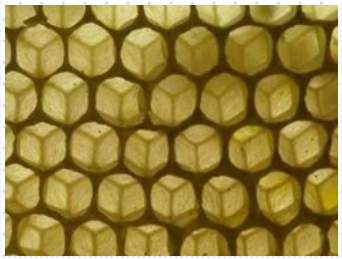
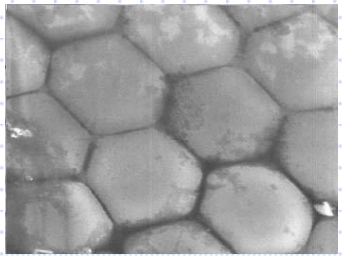
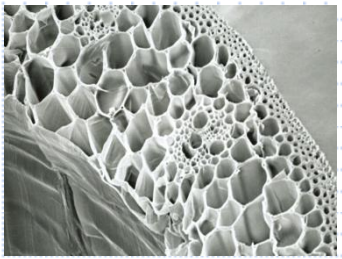

Possible applications in **automotive**, **aerospace**, **ship**, **rail** and other industries.









Cellular materials

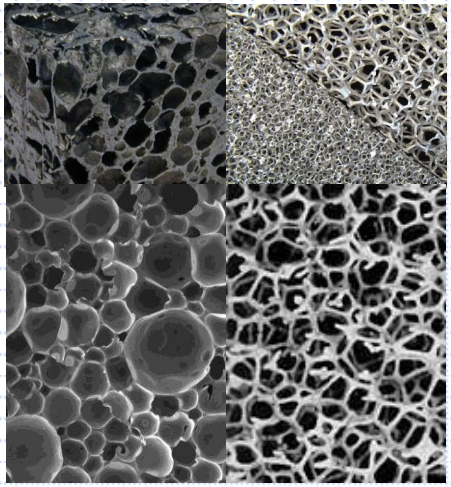

- mechanical properties determined by the microstructure (geometry, closed or open cells) and base material;
- characteristic stress-strain behaviour under compressive loading.

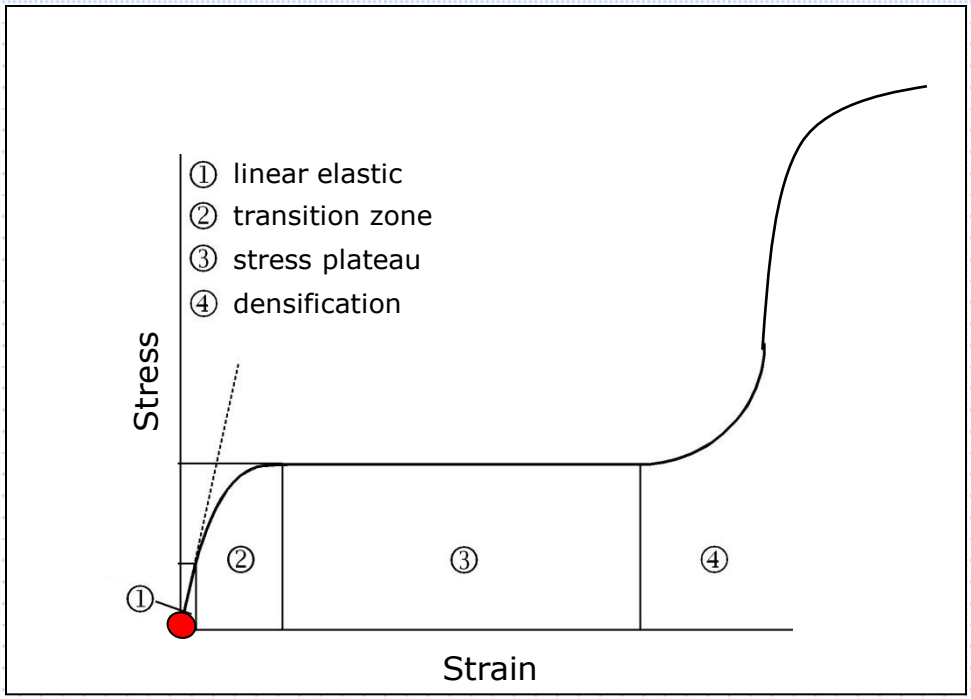

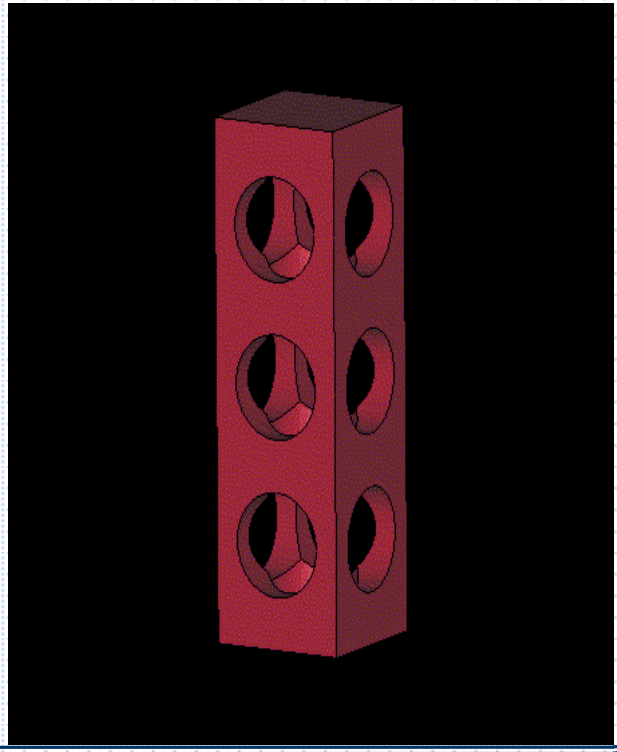

Problem statement

- to determine **mechanical behaviour of open-cell cellular structures**;
- to evaluate the **influence of fluid pore fillers on cellular structure global behaviour**;

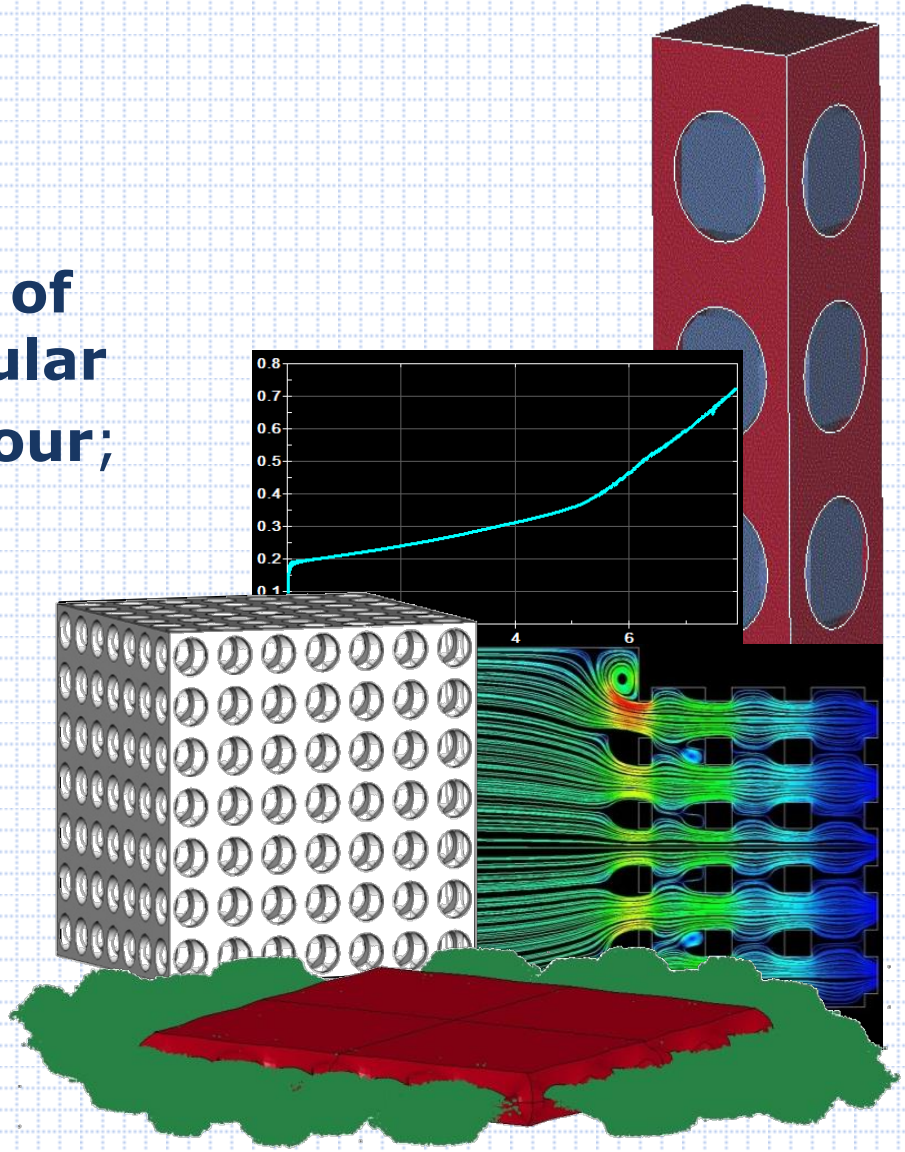

Regular open-cell cellular structure data

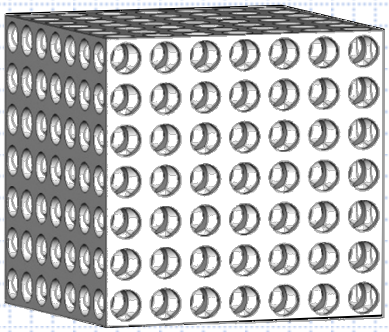

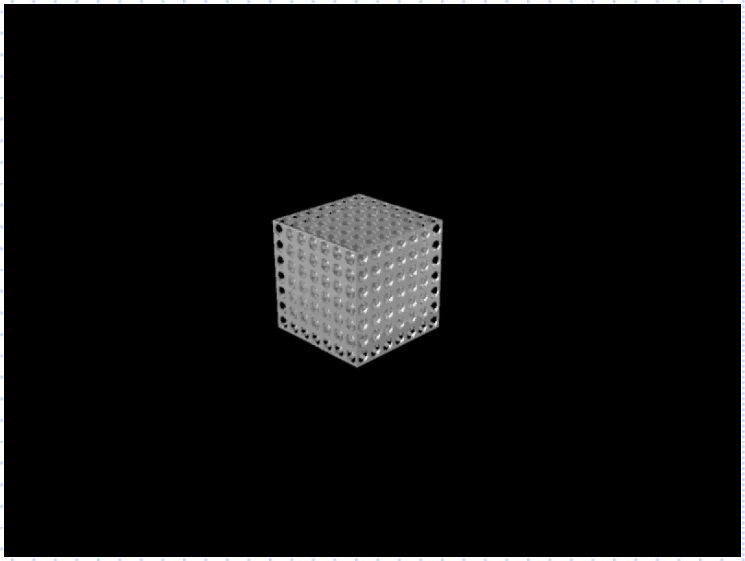

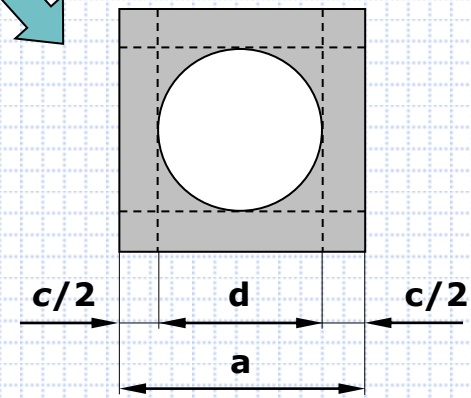

a	d	ρ/ρ_0
4.5	3.0	0.37
4.0	3.0	0.27
3.5	3.0	0.16

Experimental testing

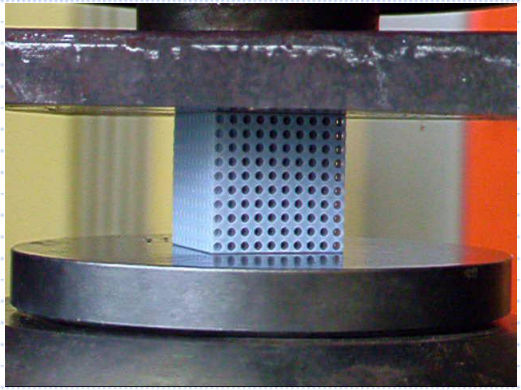

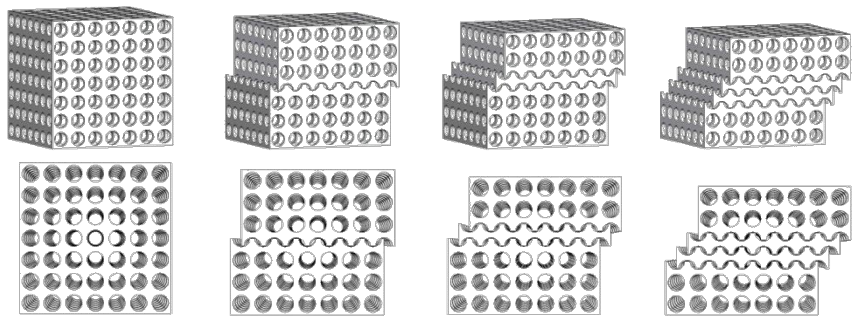

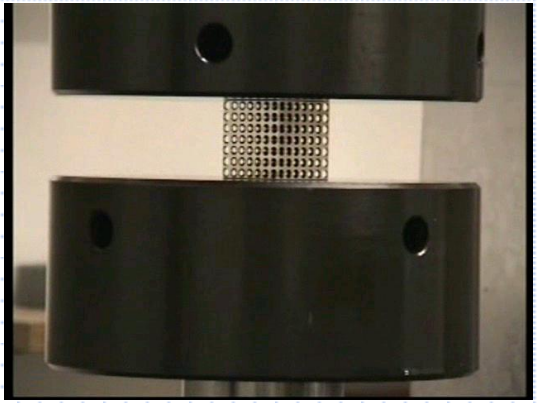

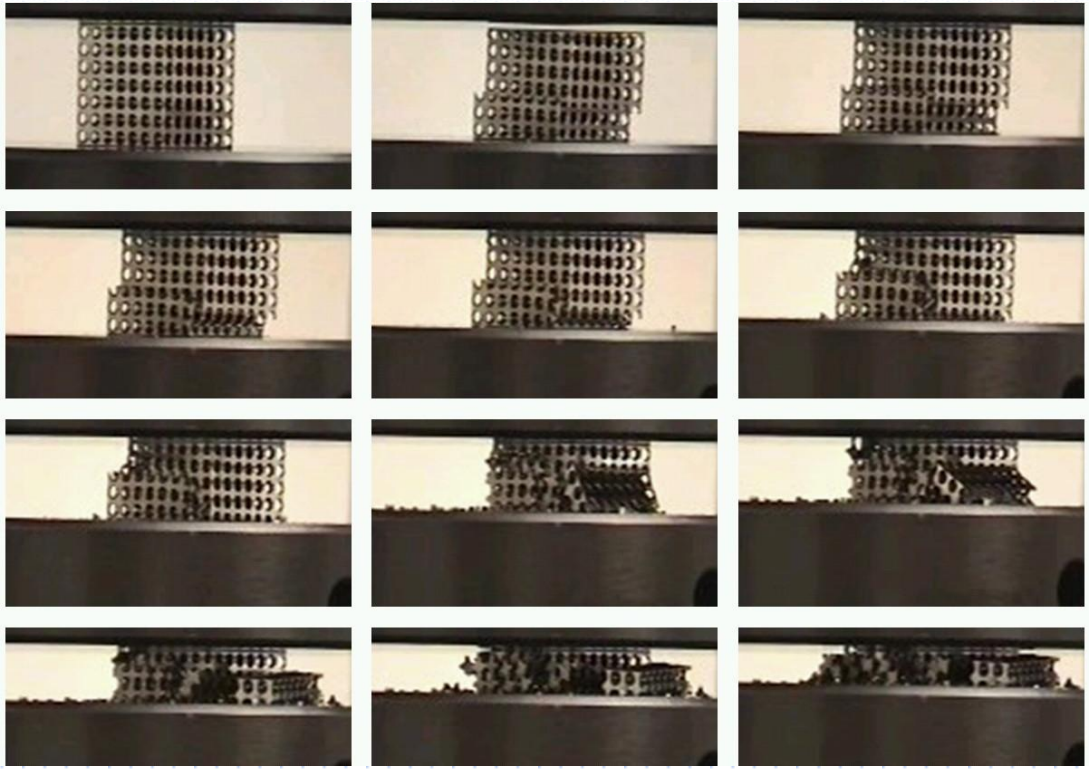

Influence of the pore filler

- **polymer FullCure**

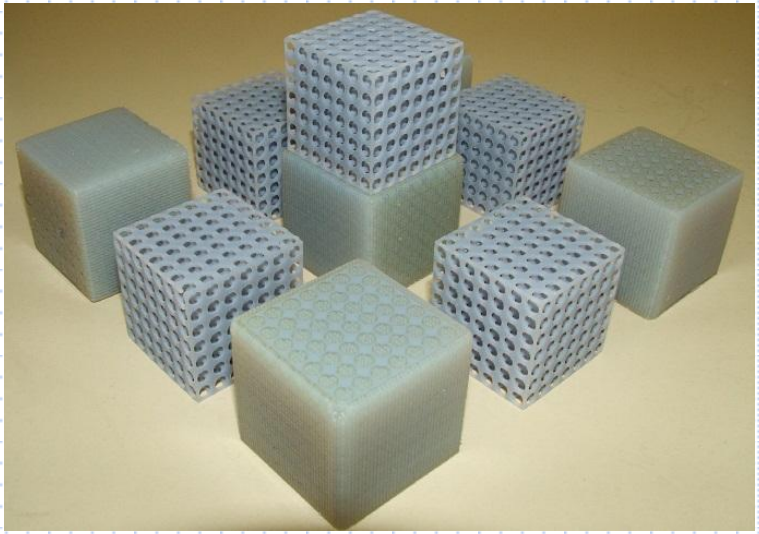

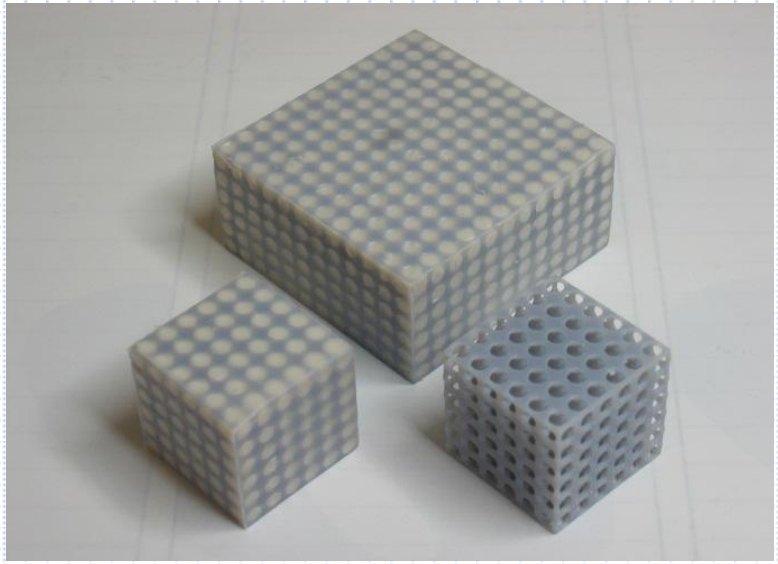

- **silicon**

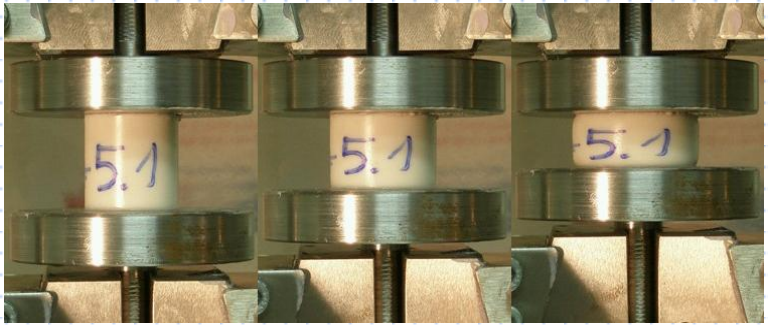

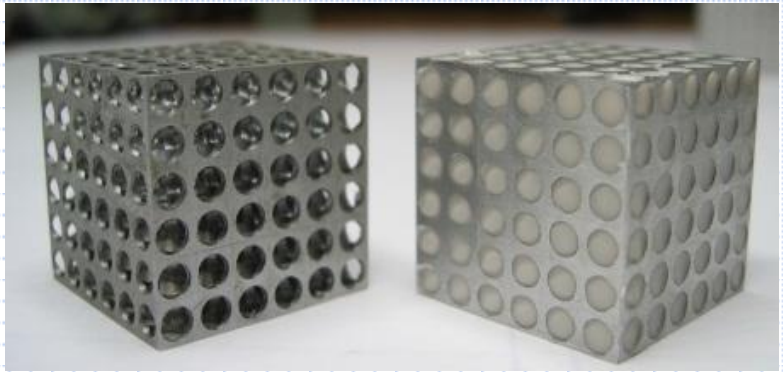

Computational modelling

- **size of the model:** 2 to 8 cells per edge
- **base material:** polymer
- **fluid pore filler:** silicon
- **loading:** displacement controlled
- **constraints:** symmetry boundary conditions
- **contact definition:** automatic single surface
- **material characterisation:** strain rate sensitivity

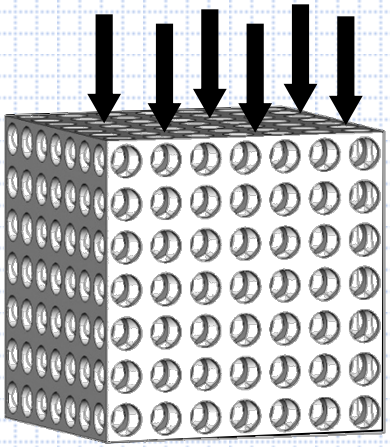

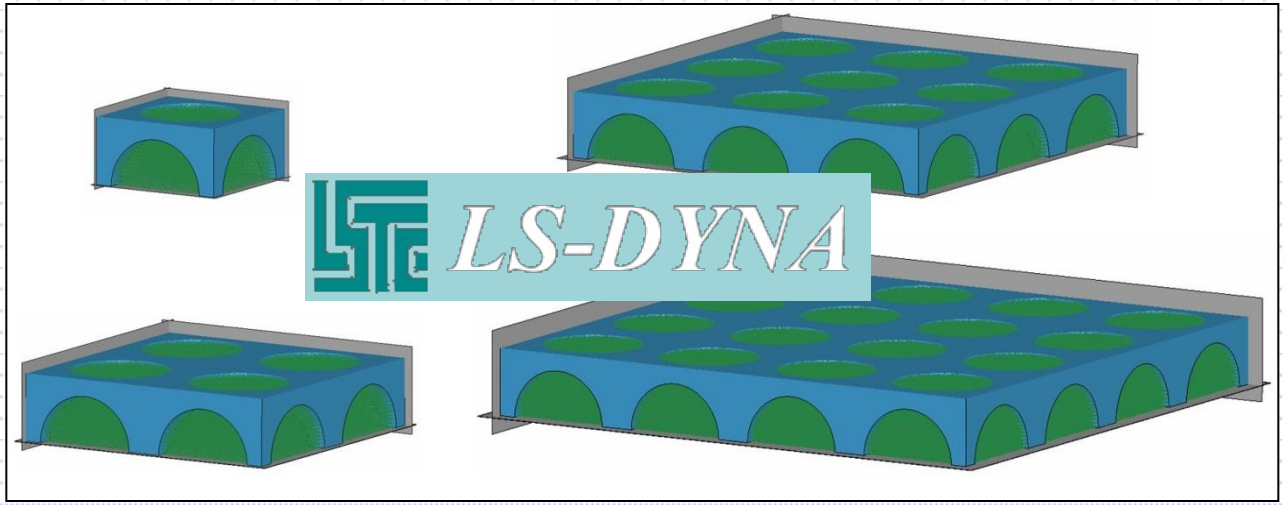

Different computational formulations

- Lagrangian formulation

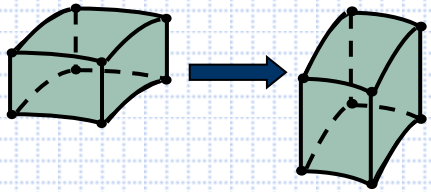

- Eulerian formulation

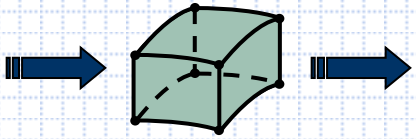

- Lagrange-Eulerian formulation (ALE)

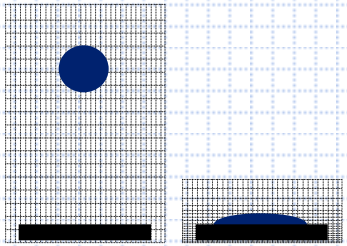

- Smoothed Particle Hydrodynamics (SPH)

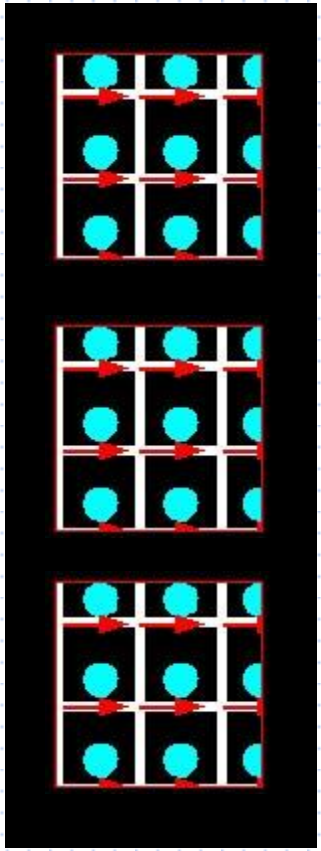

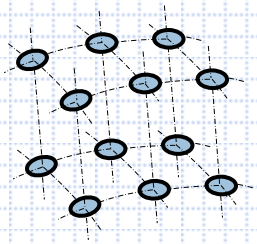

SPH = Smoothed Particle Hydrodynamics

- Integral representation (kernel approximation)

$$f(x) = \int f(x') \cdot \delta(x - x') \cdot dx'$$

Dirac Delta function $\delta(x - x') = \begin{cases} 1 & x = x' \\ 0 & x \neq x' \end{cases}$

$$f(x) \approx \int f(x') \cdot W(x - x', h) \cdot dx'$$

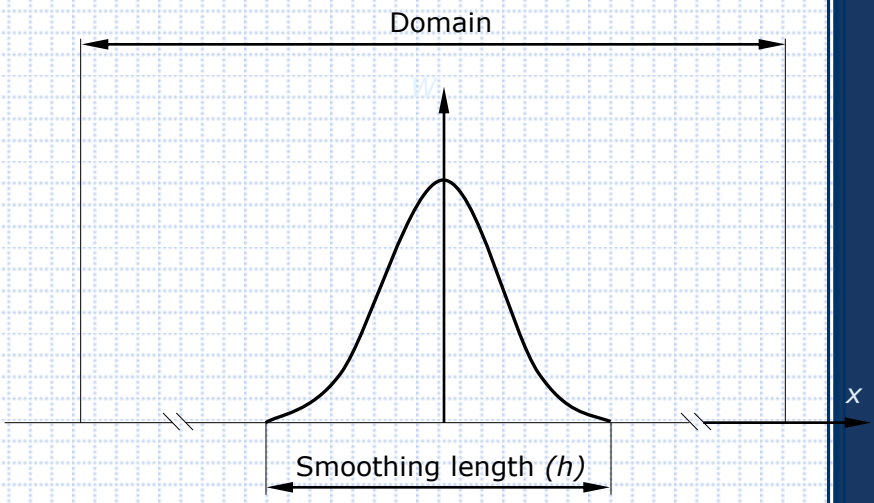

- Particle approximation

$$f(x) \approx \sum_{j=1}^{N} f(x_j) \cdot W(x - x_j, h) \cdot \Delta V_j$$

$$m_j = \Delta V_j \cdot \rho_j$$

$$f(x_i) \cong \sum_{j=1}^{N} \frac{m_j}{\rho_j} f(x_j) \cdot W_{ij}$$

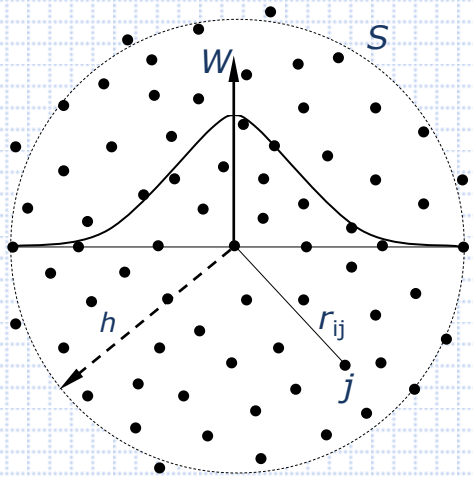

SPH = Smoothed Particle Hydrodynamics

- smoothing length (h)

$$\frac{dh}{dt} = \frac{1}{3} \cdot h \cdot div(v)$$

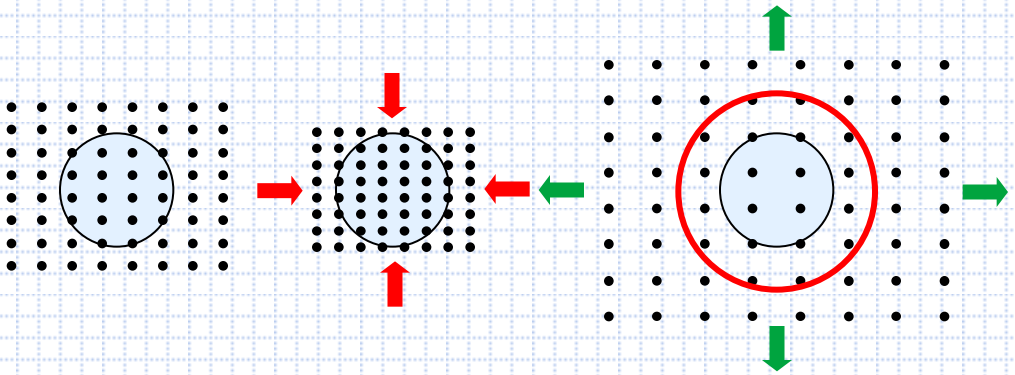

- neighbour search (bucket sort)

~~N·(N-1)~~

N·log(N)

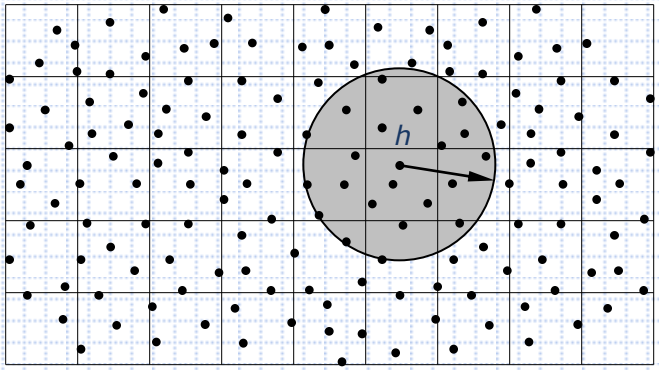

Fluid filler modelling

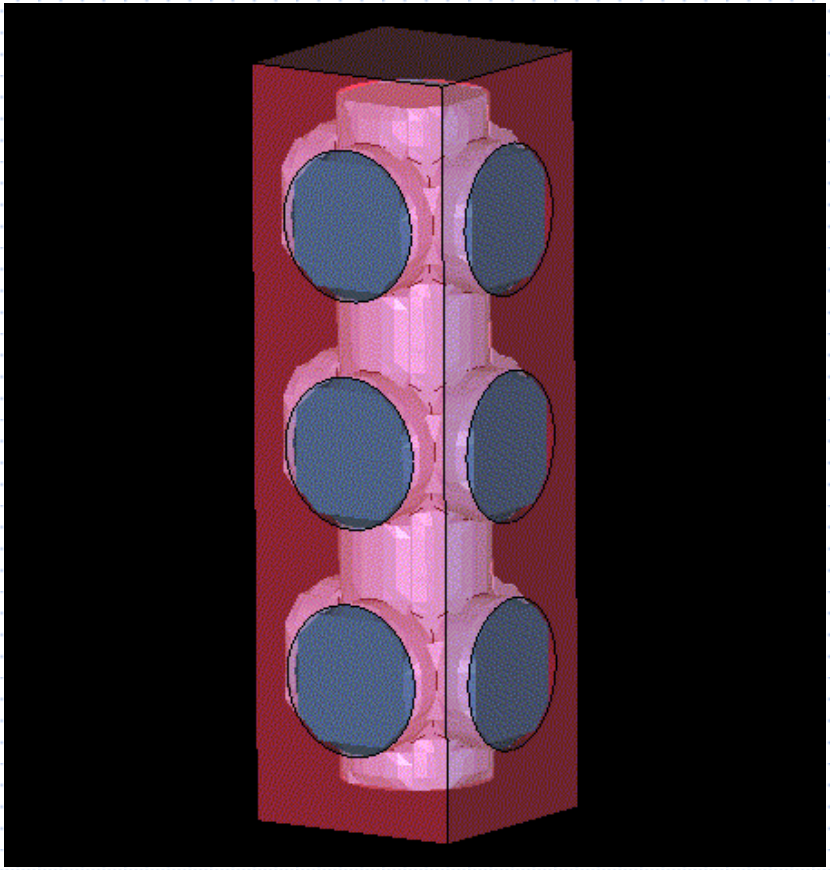

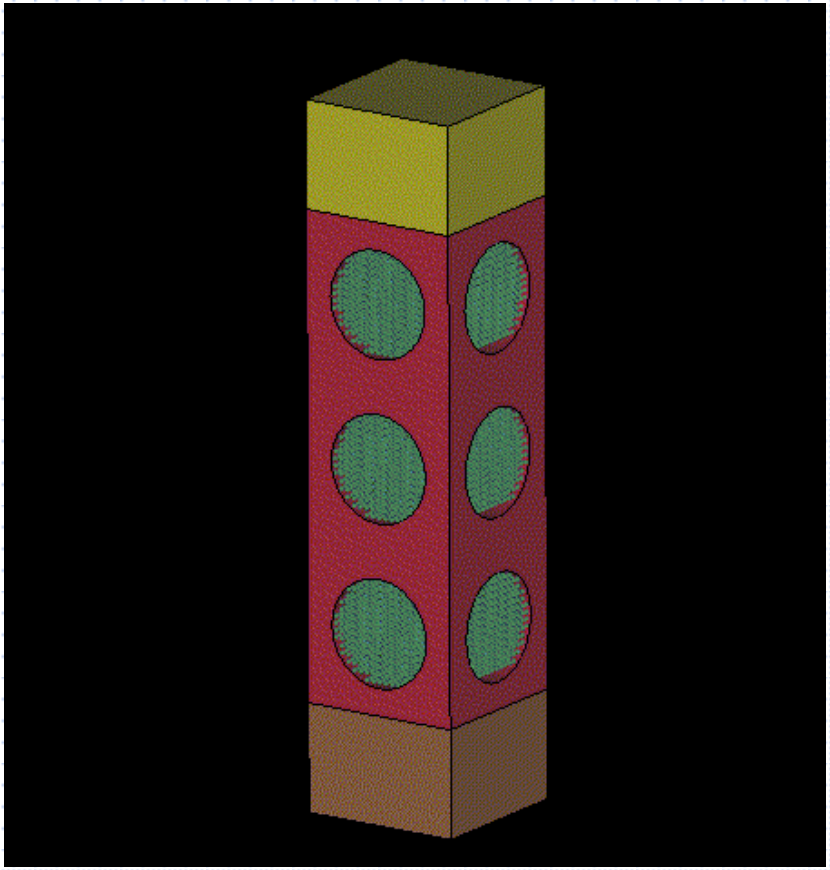

ALE

Arbitrary Lagrange-Eulerian

SPH

Smoothed Particle Hydrodynamics

ALE and SPH results comparison

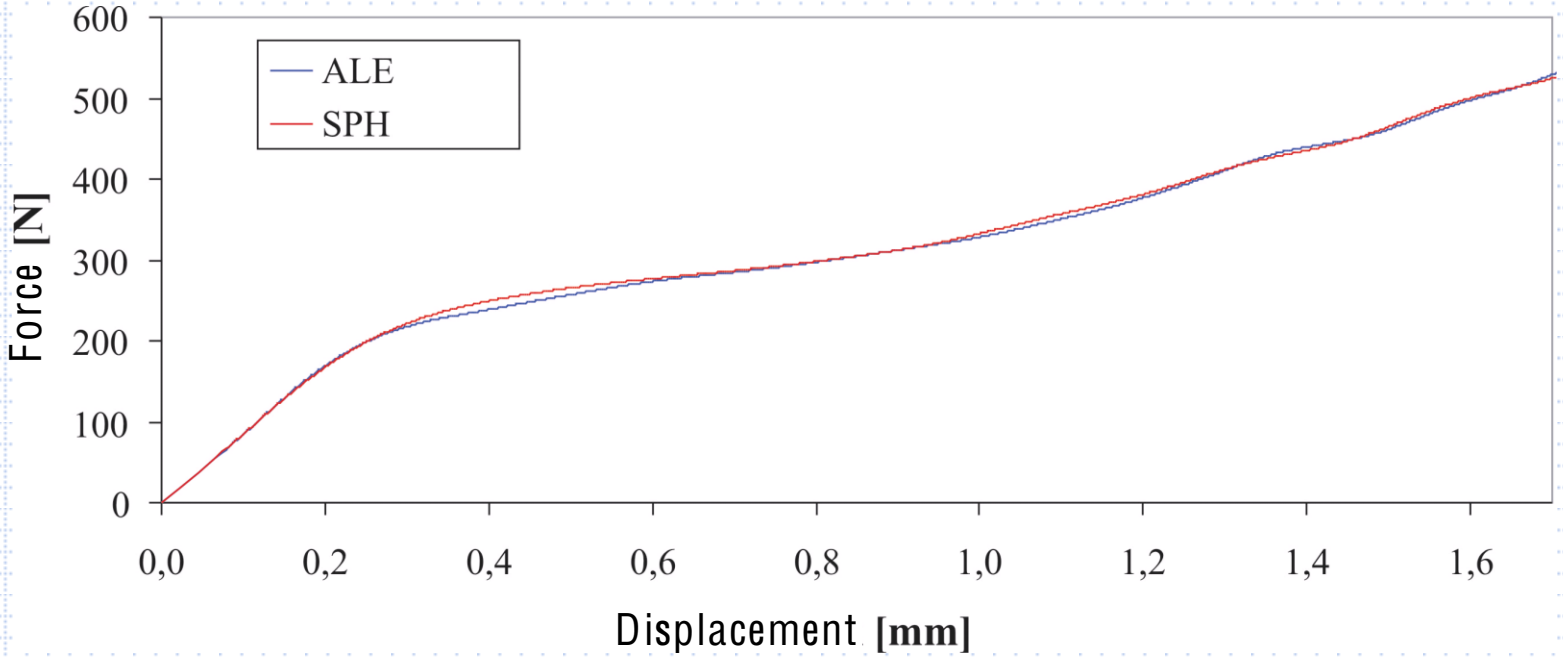

Model	Number of elements (particles)				Comput. time [min]
	Cellular structure	Filler (water)	Outer medium (air)	Total number	
ALE	3176	17408	52224	74356	**346**
SPH	3176	16692	0	19868	**223**

Fluid flow verification

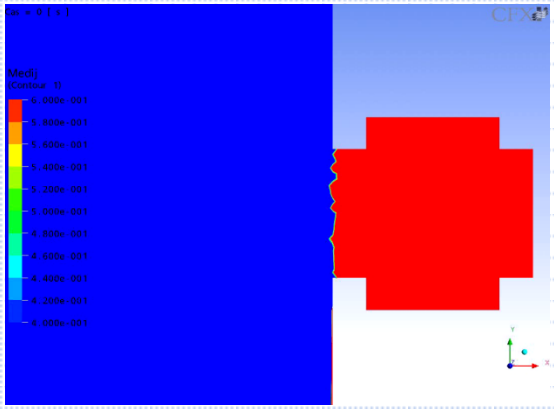

CFX

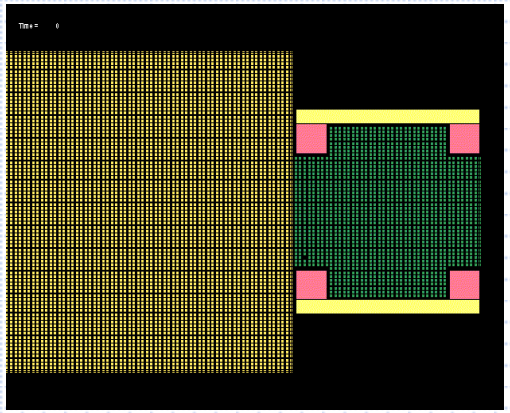

LS-DYNA

LS-DYNA

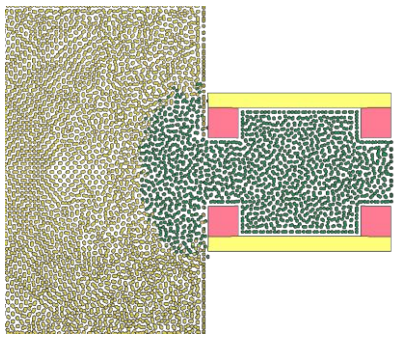

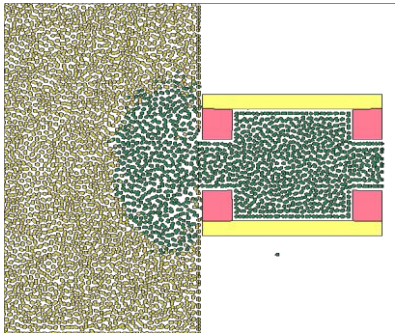

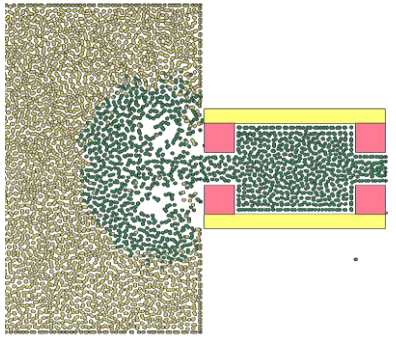

CFX

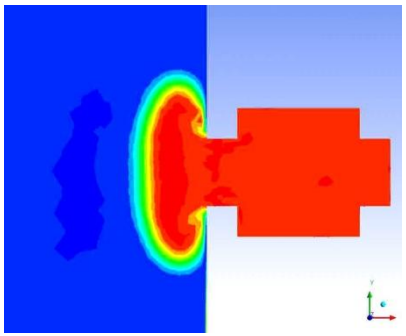

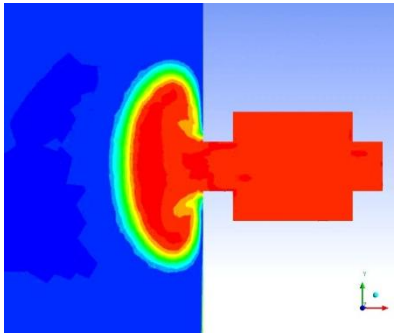

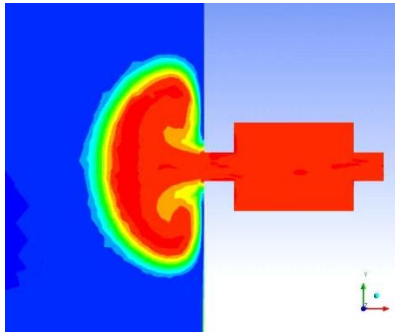

t = 0,3 ms t = 0,4 ms t = 0,5 ms

Computational simulations

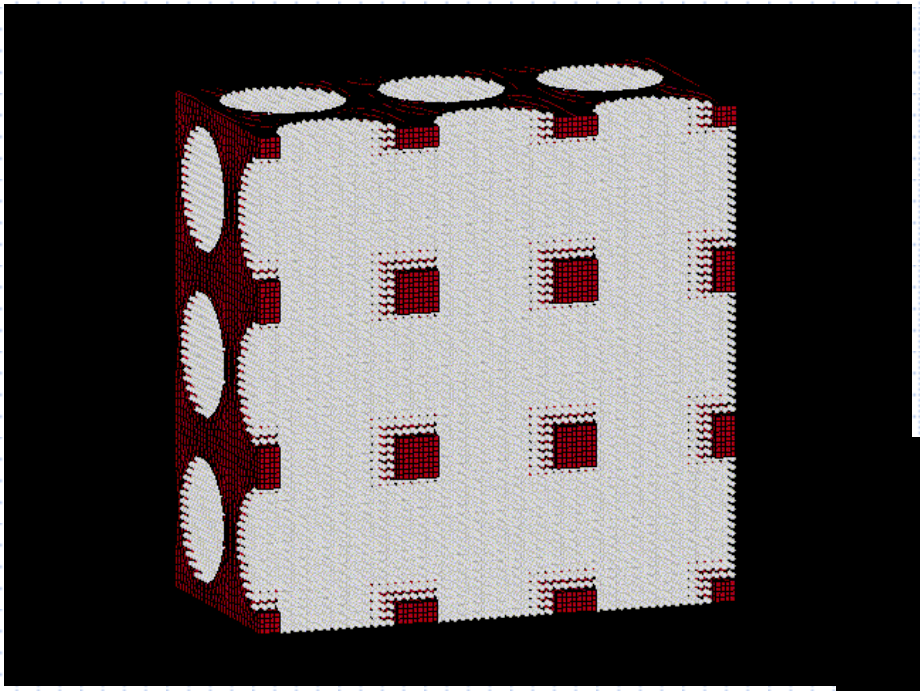

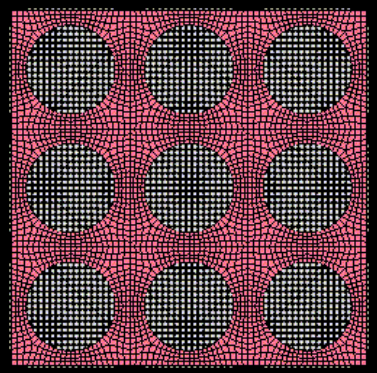

ALE and SPH results comparison

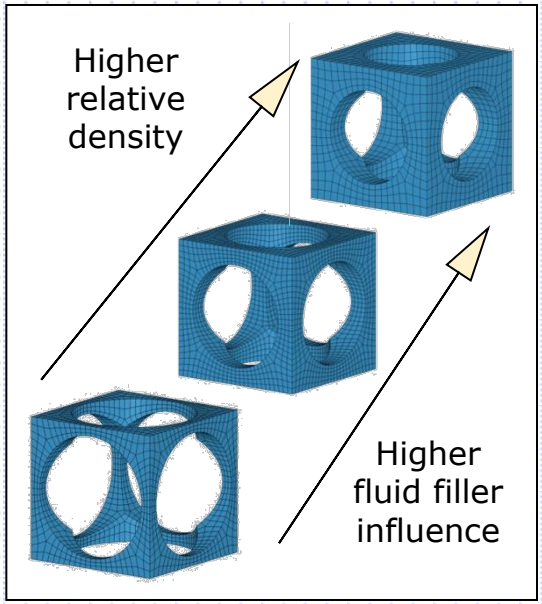

- influence of the filler is higher at higher relative densities of cellular structure;
- increasing the filler's viscosity increases the cellular structure global stiffness;

Problem statement and experimental setup

- PMMA container is filled with water.
- The SEP explosive set in the PVC pipe, positioned at the water surface, is used as booster explosive for shock wave generation and initiated by electric detonator.
- Aluminum foam is placed at the bottom of the water container.

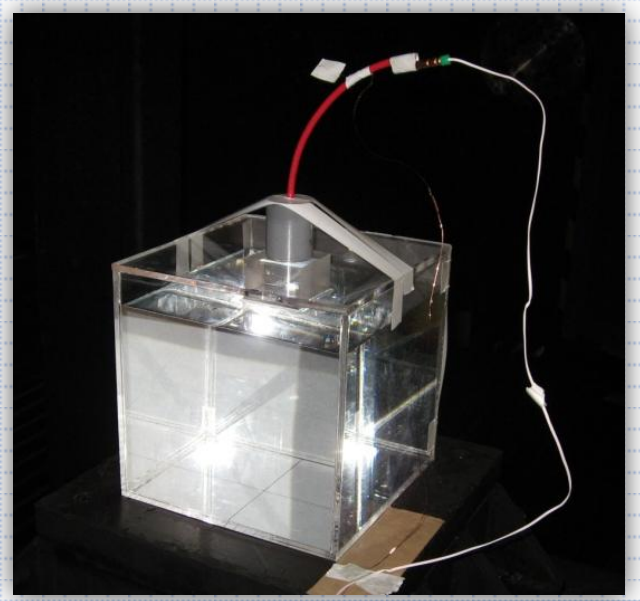

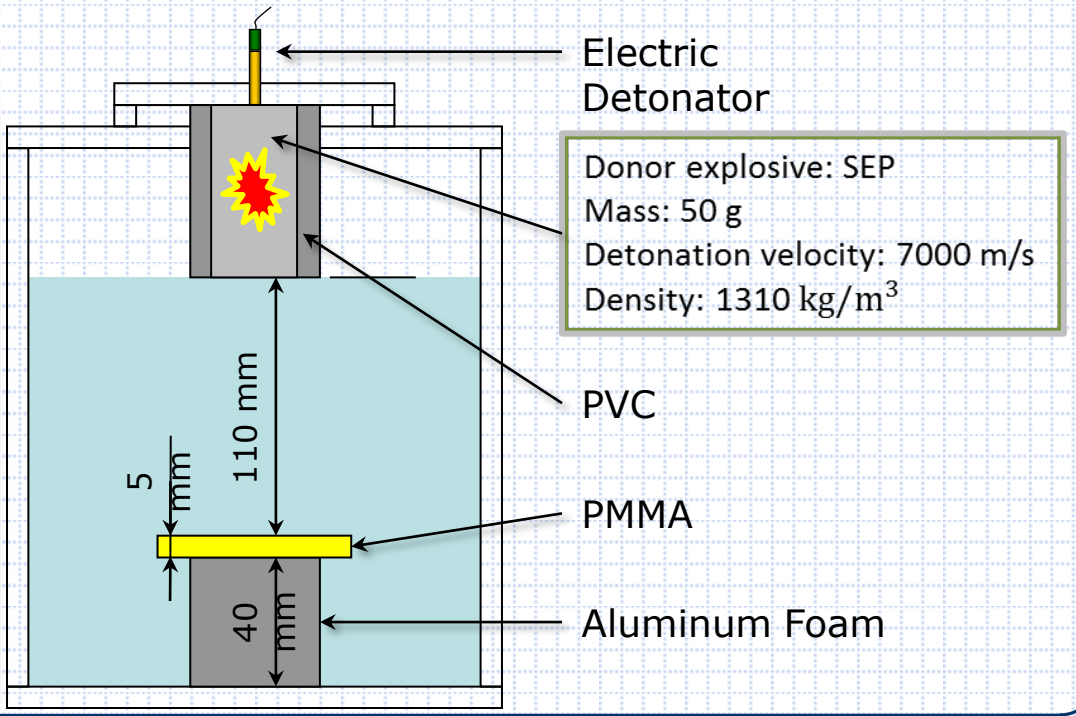

Experimental setup

The **shadowgraph method** was used to observe the generation of shock wave and its influence on the cellular structure at the **Shock Wave and Condensed Matter Research Center, Kumamoto University**.

High speed video Camera
-HPV-1-
（SHIMADZU CORPORATION）

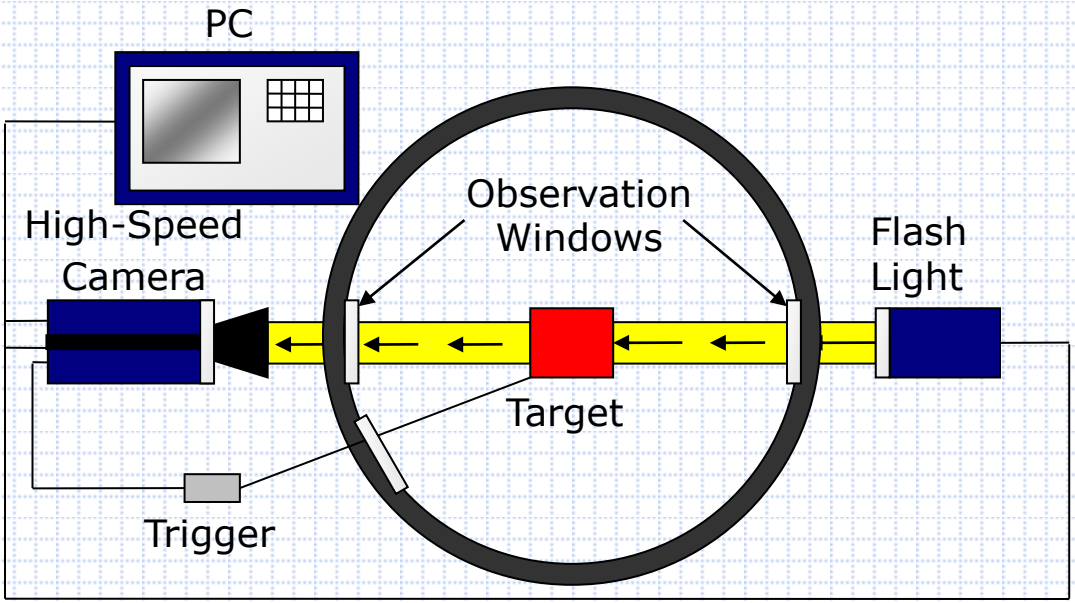

Experimental results

The following video was recorded using the **shadowgraph system** and a high speed video camera HPV-1 with a frame rate of 500.000 FPS and an image resolution of 320 x 260 pixels.

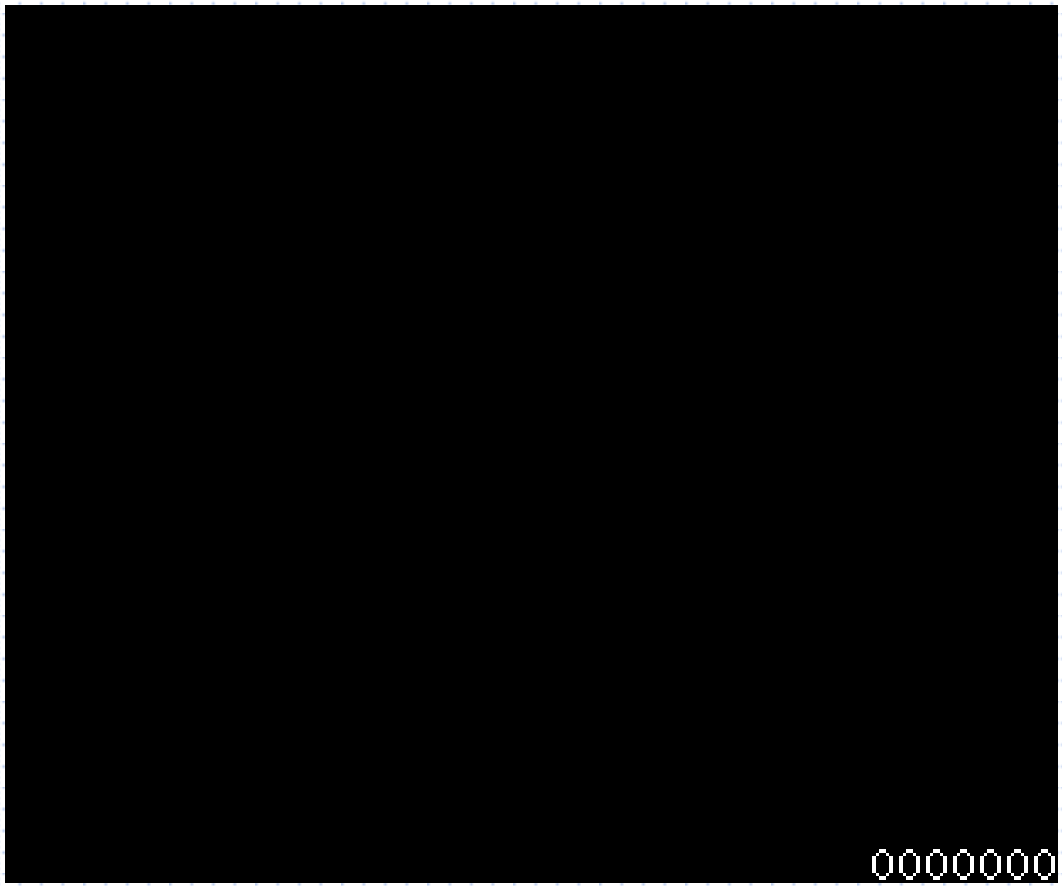

Experimental results

The speed of the shock wave was determined by analyzing the images taken during the experiment. The maximum value of the shock wave speed equaled to approximately **2700 m/s**. The accuracy was limited by the pixel size and was approximately +/-250 m/s.

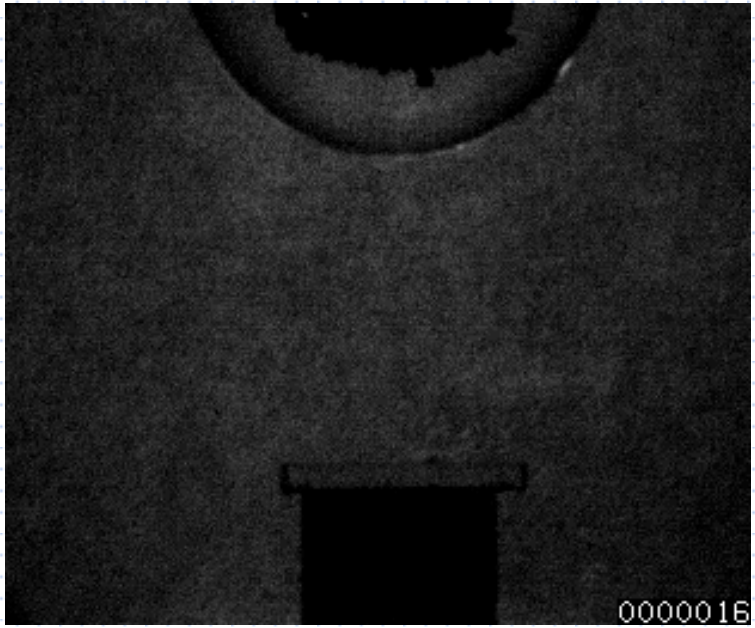

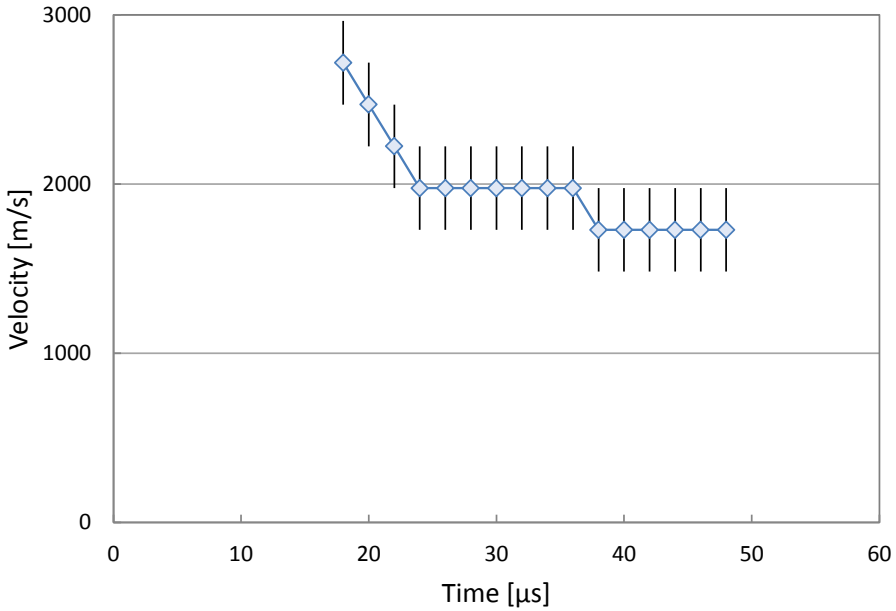

Computational simulations of shock wave

First a simulation of shock wave propagation through water without a foam model was performed – only a quarter of the volume was modeled due to symmetry.

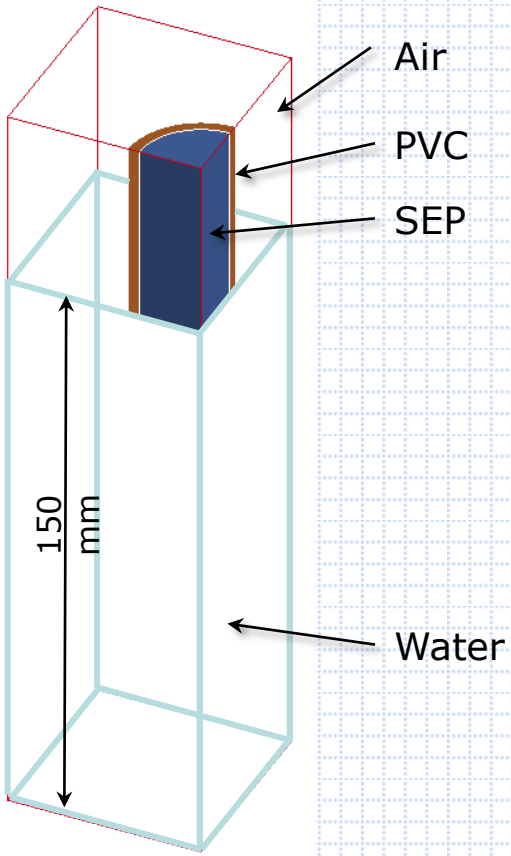

Parts modeled with an Eulerian mesh:

- a Jones-Wilkins-Lee (JWL) equation of state was used for the explosive SEP;
- a Mie Gruneisen equation of state was used for the water;
- a linear polynomial equation of state was used for the air.

Part modeled with Lagrangian mesh:

- a piecewise-linear plasticity constitutive model with failure was used for the PVC;
- a fluid-structure interaction interface was used on the boundaries of the PVC mesh.

Computational simulations of shock wave

The left video represents the expansion of the explosion gases (blue) while the right video represents the shock wave pressure field propagation.

Red Color – Air

Blue Color – SEP

Green Color- Water

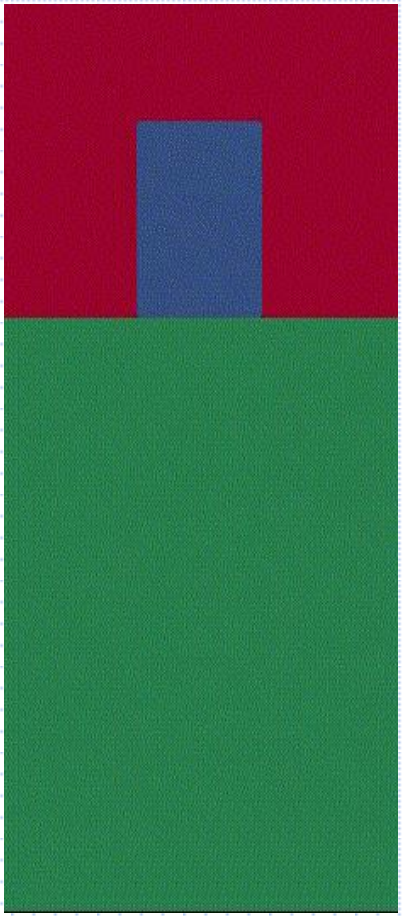

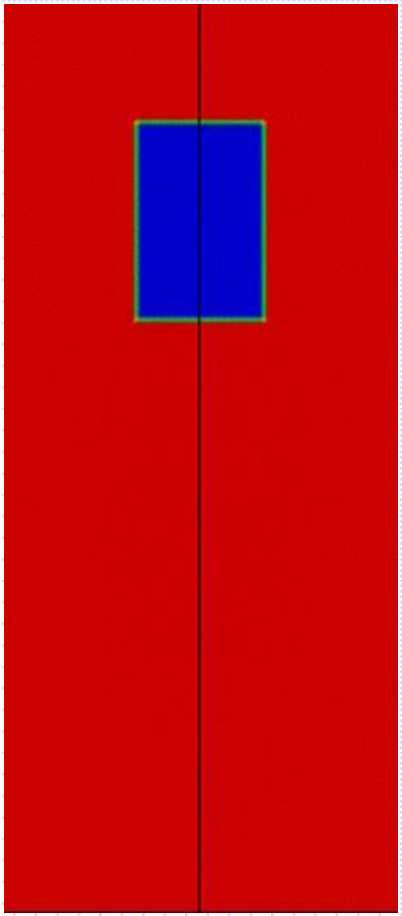

Computational simulations of shock wave

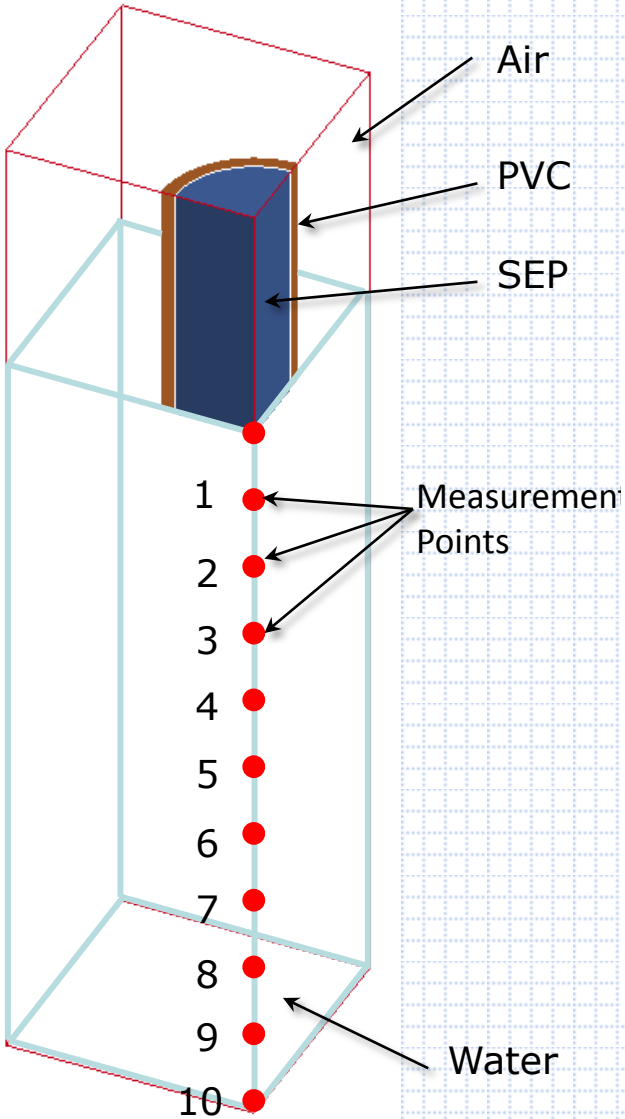

Pressure history at selected points

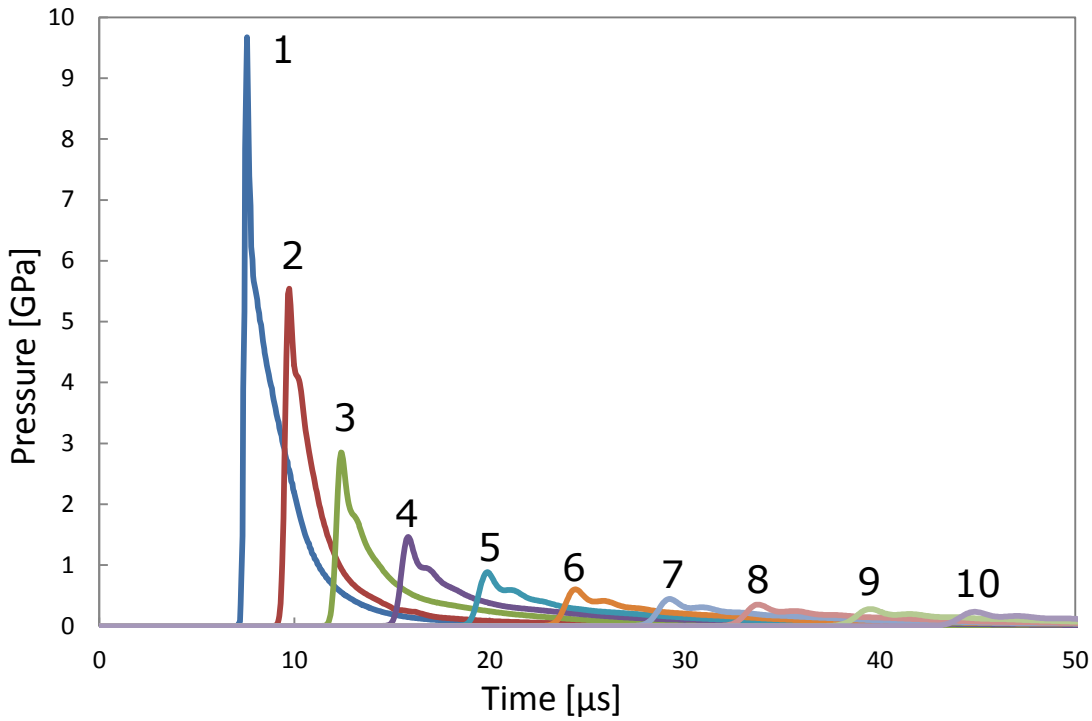

Shock wave speed comparison

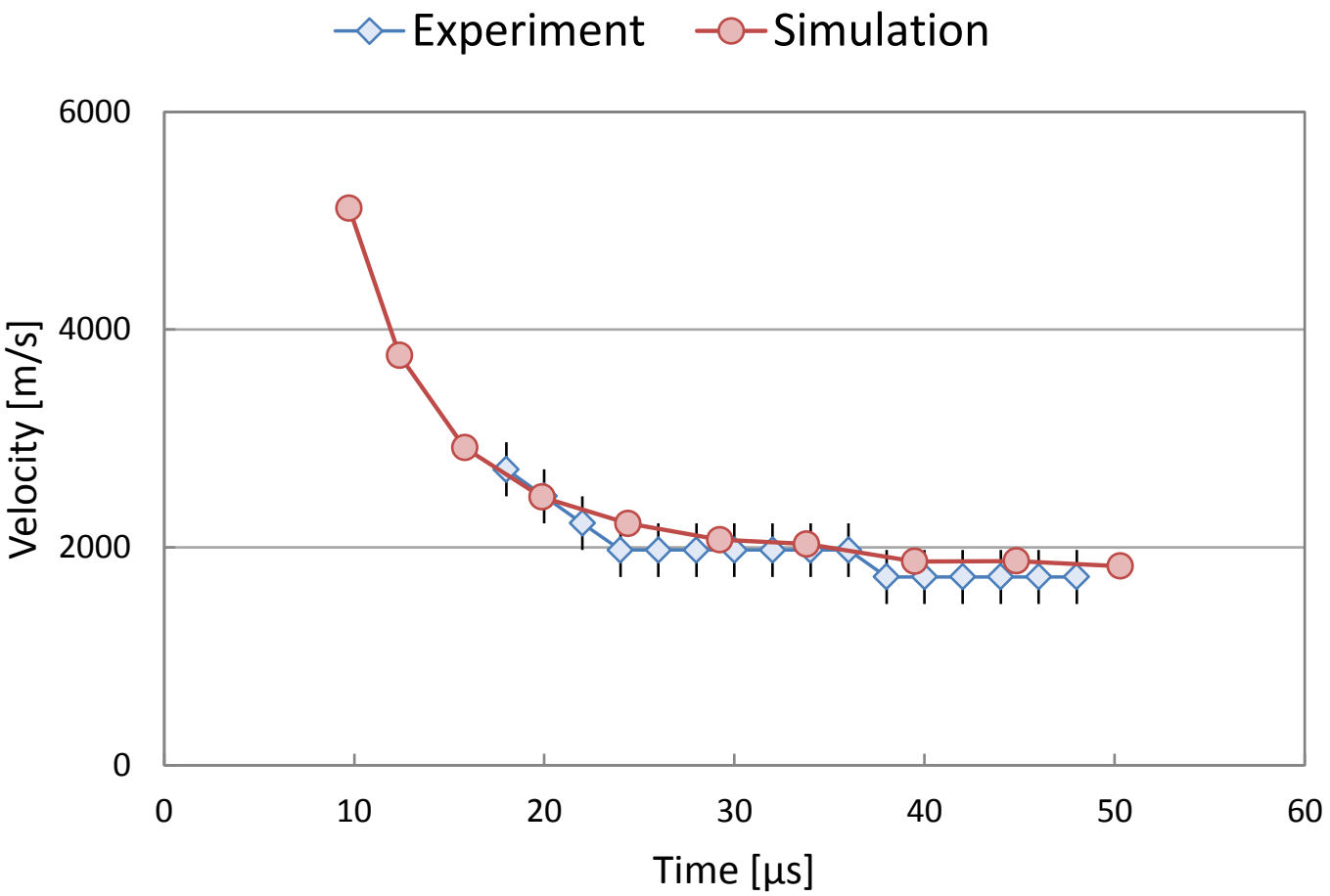

Comparison of the results shows a good correlation between the experimental and simulation results considering the measurement error.

Computational simulation with aluminium foam

In order to simulate the explosion effects on the deformation behavior of the open-cell aluminum foam, a **homogenized foam model** was added to the simulation.

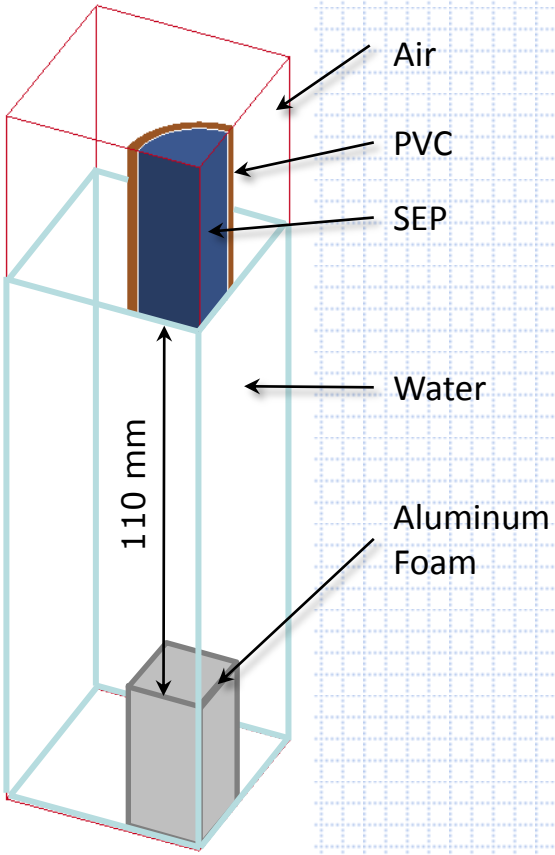

Model 1	Model 2	Model 3
The foam was modeled using **Lagrangian mesh** with a piecewise-linear plasticity constitutive model	The foam was modeled using **Lagrangian mesh** with a piecewise-linear plasticity constitutive model	The foam was modeled using **Eulerian mesh** with a piecewise-linear plasticity constitutive model
Water domain was modeled **inside the foam**.	**Air domain** was modeled **inside the foam**.	

Deformation of homogenized cellular model

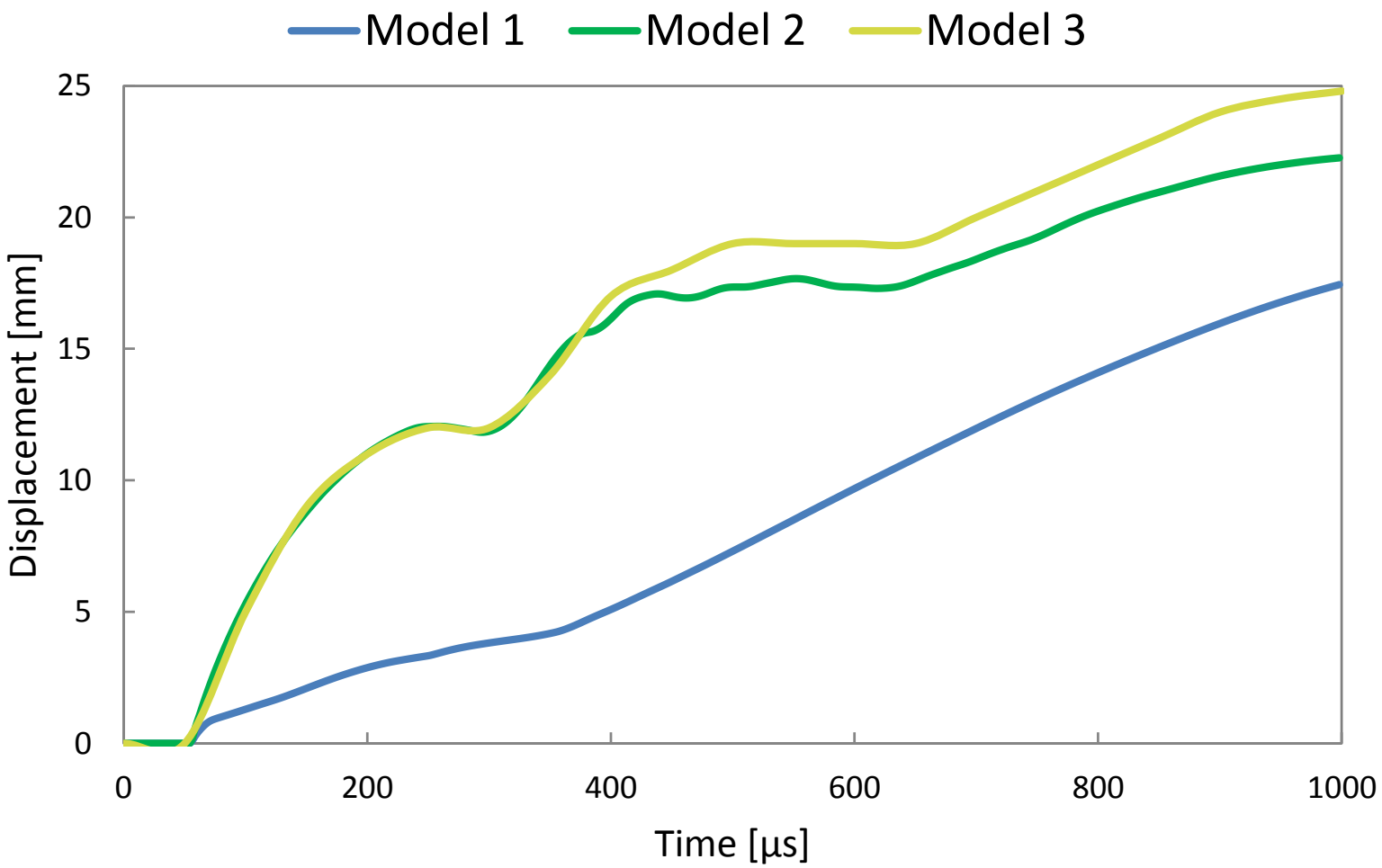

The model 3 (Eulerian foam model) exhibited the lowest stiffness while the highest stiffness was observed for model 1 (Lagrangian mesh filled with water).

Lattice model of the aluminium foam

In the following simulations the aluminum foam was modeled with a **lattice model to represent irregularity of the structure**. The foam cell edges were modeled with beam finite elements and their topology was created using a developed algorithm based on Voronoi 3D regions.

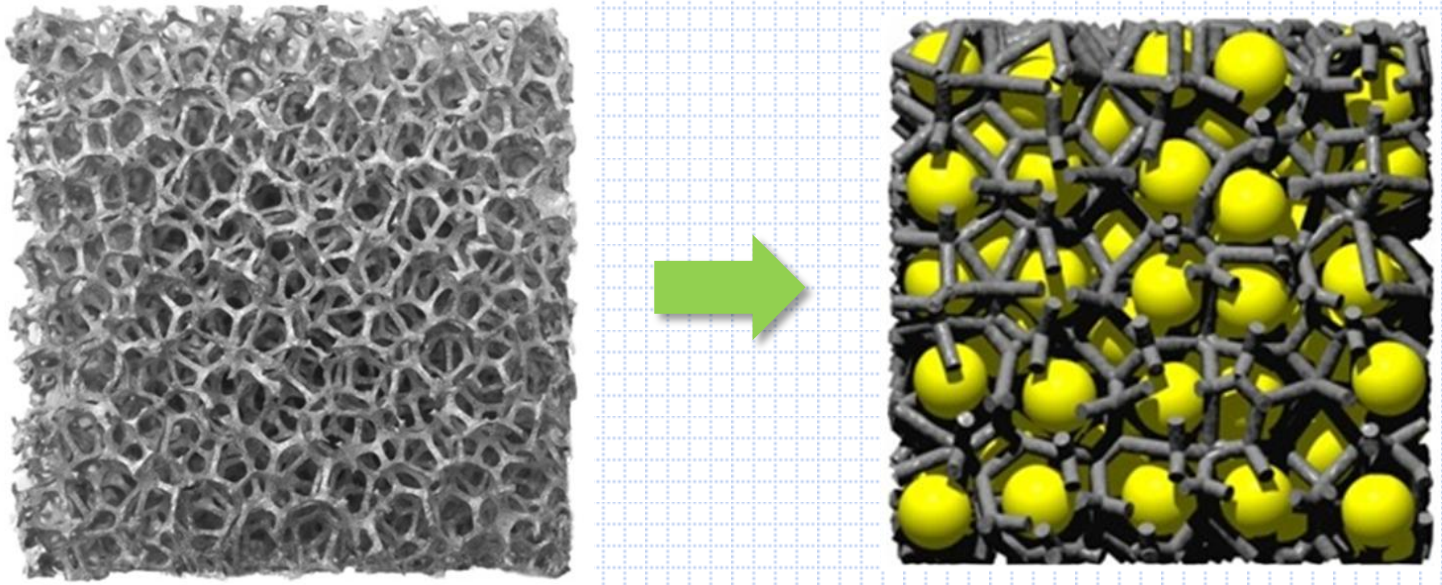

Computational simulations with lattice models

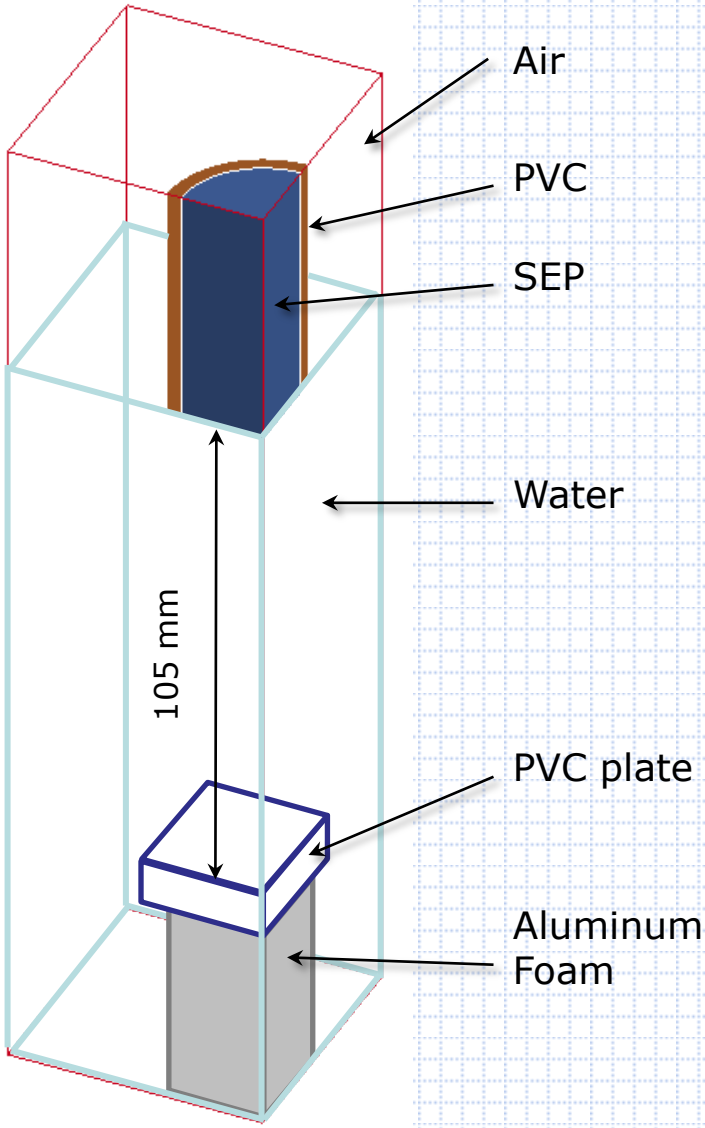

Three different relative densities of the aluminum foam were considered: 5, 10 and 15 %.

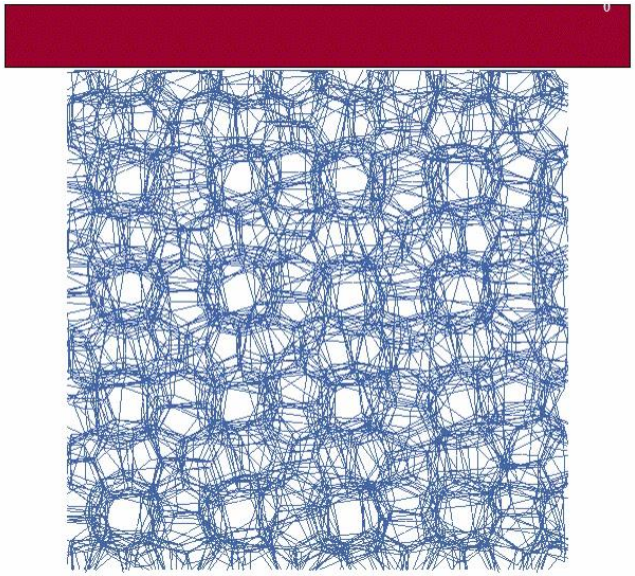

CONCLUSION

- Engineers can now perform multiphysics computational analysis as a routine part of product development in its early stages.
- Companies and individuals that previously could not afford to invest in this technology can now readily take advantage of multiphysics computational simulations.
- Multiphysics has become a strategic tool for system engineering methodologies that account for all relevant physical phenomena that influence design and thus enable companies to develop innovative, winning products in less time and at lower cost.